Journal of Theoretical Biology 271 (2011) 181–201

Contents lists available at ScienceDirect

Journal of Theoretical Biology

journal homepage: www.elsevier.com/locate/yjtbi

Highly pathogenic avian influenza outbreak mitigated by seasonal low pathogenic strains: Insights from dynamic modeling

L. Bourouiba [a,*], A. Teslya [b], J. Wu [c,d]

[a] Department of Mathematics, Massachusetts Institute of Technology, 77 Massachusetts Avenue, Cambridge, MA 02139-4307, USA
[b] Department of Mathematics, Ryerson University, 350 Victoria St., Toronto, Canada ON M5B 2K3
[c] Department of Mathematics and Statistics, York University, 4700 Keele Street, Toronto, Canada ON M3J 1P3
[d] Centre for Disease Modelling, York University, 4700 Keele Street, Toronto, Canada ON M3J 1P3

ARTICLE INFO

Article history:
Received 30 March 2010
Received in revised form
28 October 2010
Accepted 8 November 2010
Available online 10 December 2010

Keywords:
H5N1
Highly and low pathogenic avian influenza
Partial immunity
Environmental transmission
Contact transmission

ABSTRACT

The spread of highly pathogenic avian influenza (HPAI) H5N1 remains a threat for both wild and domestic bird populations, while low pathogenic avian influenza (LPAI) strains have been reported to induce partial immunity to HPAI in poultry and some wild birds inoculated with both HPAI and LPAI strains. Here, based on the reported data and experiments, we develop a two-strain avian influenza model to examine the extent to which this partial immunity observed at the individual level can affect the outcome of the outbreaks among migratory birds in the wild at the population level during different seasons. We find a distinct mitigating effect of LPAI on the death toll induced by HPAI strain, and this effect is particularly important for populations previously exposed to and recovered from LPAI. We further investigate the effect of the dominant mode of transmission of an HPAI strain on the outcome of the epidemic. Four combinations of contact based direct transmission and indirect fecal-to-oral (or environmental) routes are examined. For a given infection peak of HPAI, indirect fecal-to-oral transmission of HPAI can lead to a higher death toll than that associated with direct transmission. The mitigating effect of LPAI can, in turn, be dependent on the route of infection of HPAI.

1. Introduction and background

Avian influenza is caused by a virus frequently affecting wild birds and poultry with high variation from one species to another. The range of symptoms caused by the virus in chicken populations is often used to classify the virulence of avian influenza viruses. The mild form, referred to as low pathogenic avian influenza (LPAI), can cause mild to no symptoms and is often detected in the wild. Highly pathogenic avian influenza strains are highly contagious and can cause systemic infection and high mortality in poultry (up to 100% poultry mortality within days). The HPAI strains are caused by H5 and H7 subtypes of type A influenza virus (e.g. Alexander, 2007; Lucchetti et al., 2009; Swayne and Suarez, 2000). Milder versions of H5N1 cases have been reported and have induced low mortality among animals since the 1990s; however, in 2005, a new highly pathogenic strain of H5N1 virus began to have unprecedented deadly effects on various bird species, including industrial poultry and domesticated and migratory wild birds. In 2005, such outbreaks in Asia led to the culling of up to 150 million domestic birds resulting in billions of dollars in losses (Gilbert et al., 2008). Despite the increasing number of human cases (489 cases reported to WHO from 2003 to 2010 (WHO, 2010)), the human-to-human transmission of the current HPAI strain remains rare (e.g. WHO, 2008).

1.1. Effect of low pathogenic strains on high pathogenic epidemics: observations

Strains of low pathogenic avian influenza (LPAI) can induce partial immunity to HPAI in poultry and wild bird populations. However, the extent to which this partial immunity observed at the individual level in experimental studies can affect the outcome of an outbreak among birds at the population level remains to be clarified and is one of the subjects of this study.

In Hong Kong's 1997 H5N1 virus outbreak, most chickens did not show clinical signs despite a 20% prevalence. Documentation of the outbreak indicates that chickens in most markets shed virus via cloacal route. At the time, the second most prevalent virus in the market was the LPAI H9N2, which was isolated to about 5% of the chickens examined. Distinguishable lineages of H9N2 and H5N1 were present, and these led to a number of studies striving to learn how infection with LPAI strain can affect a subsequent infection by H5N1.

Seo and Webster (2001) argued that the H9N2 infection caused a cross-immunization in chicken, leading to a reduction of clinical

* Corresponding author.
E-mail addresses: lbouro@mit.edu (L. Bourouiba), ateslya@ryerson.ca (A. Teslya), wujh@mathstat.yorku.ca (J. Wu).

0022-5193/$ - see front matter © 2010 Elsevier Ltd. All rights reserved.
doi:10.1016/j.jtbi.2010.11.013

signs and death rates. To test their theory, they considered a group of chickens infected by the LPAI H9N2 influenza virus. They found that the group infected by the H5N1 within 30 days of inoculation by LPAI had a 100% survival rate, with low to undetectable viral shedding and suppressed clinic signs. As time between the two infections grew above 30 days, this effect started to fade and HPAI lethality was reported. By 70 days post LPAI infection, 4 out of 10 birds died when infected by H5N1. The results of this study suggest that the acquired immunity due to a previous LPAI is only temporary.

Pasick et al. (2007) immunized Canada Geese with H5N2 virus prior to infecting them with H5N1. Their results were similar to those of Seo and Webster (2001). A previous infection by H5N2 induced a reduction in H5N1-induced lethality and reduced or suppressed H5N1 clinical signs of infection. Adult birds responded to H5N2-immunization and subsequent H5N1 infection better than juveniles, and the survival rate for both adult and juvenile birds was 100%. The study by Kalthoff et al. (2008), focusing on Mute Swans, established that the birds with specific avian influenza anti-bodies did not show symptoms upon re-infection by H5N1. Although the sample size of the experiment of this study was small (two birds), the results are in line with the conclusions of Seo and Webster (2001) and Pasick et al. (2007). These studies support the hypothesis that pre-exposure of birds to a LPAI virus strain minimizes the mortality and symptoms of a subsequent H5N1 infection occurring soon after, although the pre-exposed birds can still get infected with H5N1 and are able to shed the virus asymptomatically.

The first goal of this study is to investigate how pre-exposure to LPAI impacts the epidemic outcome in flocks of migratory birds at various times of the year related to the seasonal change of the LPAI prevalence. In order to do so, we develop a mathematical model of disease dynamics focusing on capturing the clinical results reported in the literature. Two strains are considered, one LPAI strain and another HPAI strain.

1.2. Routes of transmission: direct or indirect?

Waterfowls are known to be reservoirs for avian influenza viruses (e.g. CDC, 2006; Munster et al., 2007). Ducks, shorebirds and gulls were particularly well documented for their capacity to shed LPAI virus for a long period of time, with ducks being able to shed the virus via intestinal tract for up to 4 weeks (Webster et al., 1992). LPAI peak prevalence varies from a few percent in the winter months to up to 30% during the weeks preceding the fall migration (e.g. Stallknecht, 1997).

Contrary to this mechanism, HPAI virus shedding is predominantly via respiratory tract (e.g. Brown et al., 2008; Keawcharoen et al., 2008; Globig et al., 2009; Jeong et al., 2009). These recent findings suggest that a transmission of H5N1 among wild birds should involve in large part a direct close-contact route as opposed to an indirect fecal-to-oral route. Globig et al. (2009) discussed the impact of such a finding as a possible explanation for the relatively localized and surprisingly species-limited H5N1 outbreaks observed in Germany during 2006 and 2007. Focusing on the effect of the environmental contamination by LPAI, Breban et al. (2009) suggested that the presence of the virus in the environment could account for the LPAI virus persistence in small size communities which should otherwise be cleared of the virus. The authors noted that if the size of the population is small, the environmental transmission rate becomes a key factor in the epidemic. Similarly, Rohania et al. (2009) proposed that the LPAI environmental virus transmission gives rise to dominant indirect transmission mechanisms. Using stochastic modeling, the authors showed that overlooking environmental transmission leads to missing some characteristics of the epidemics observed, such as explosiveness and duration. In light of these recent results, our second goal is to examine the impact of a higher oropharyngeal shedding for the HPAI strain on the outcome of the epidemic. In particular, we examine the impact of a changing dominant mode of transmission from indirect environmental to direct contact transmissions for HPAI H5N1 on the death-toll of the HPAI epidemic. Furthermore, we examine if the LPAI mitigating impact is also affected by the change of dominant mode of HPAI transmission.

1.3. Outline

The remainder of the paper addresses the two goals of the study as follows. The underlying modeling assumptions and description are given in Section 2 and analyzed in Section 3. The rational for the choice and evaluation of the parameters of the model are detailed in Section 4. The results of mitigating impact of LPAI on HPAI epidemic outcomes are discussed in Section 5. Finally, we discuss the roles of environmental HPAI and LPAI transmission modes in Section 6.

2. Assumptions and model formulation

The model describes the dynamics of two strains of avian influenza in a bird population. We consider the influence of a coexisting and preceding LPAI epidemic on the transmission dynamics and mortality caused by a HPAI strain suddenly introduced on a wild migratory bird population during migration. We are not concerned by the source of the HPAI, which could be a spill-over from LPAI (see discussion in Lucchetti et al., 2009) or could have been introduced by other means, such as illegal poultry trade, with various impacts (see discussion in Iwami et al., 2009, for example). Our focus is on a highly susceptible species of ducks such as the wood duck, which reacts violently to the HPAI compared to, for example, Mallards (Schaefer et al., 2009; Brown et al., 2006). The spatial location of the migrating birds and seasonality are linked. Schematically, birds spend the winter months in warmer locations, where they feed and prepare for the start of a typically "northward" spring migration to reach their "breeding ground", where they spend the summer months. It is only during the summer months that breeding occurs for a short period of time. Late in the summer or early fall, molting can occur and birds typically gather and prepare for the fall migration southward. At this time of the year the birds are gathered in large numbers and the proportion of juveniles is the highest of the year. Along the fall and spring migratory routes, the birds stop regularly to feed or rest. We refer to these stop locations as stopovers. The goal is to capture the dynamics of the epidemics occurring on stopovers along a yearly migratory route, with particular interest in the effect of previous LPAI infection on the evolution of HPAI. As discussed in Section 1.1, if significant at the population level, this effect would only be temporary, wearing off within a month or two. It is known from the literature that migratory birds (of various species) can reside on a stopover from a few days to $\approx 3-4$ months. The longest residence time is that associated with wintering and breeding (possibly molting) patches (see, for example, the satellite tracking data for bar-headed geese, Bourouiba et al., 2010, and literature about wood ducks such as Schaefer et al., 2009). Finally, the life expectancy of migratory birds can be surprisingly high, with 15–20 years for bar-headed geese or up to 15 years for wood ducks. In North America, in the wild, one can assume a life expectancy of 3–4 years for wood ducks (Schaefer et al., 2009). From the comparison of timescales involved above, we conclude that we can neglect "natural" demographics on the timescale of the LPAI–HPAI disease dynamics. Therefore, natural death and birth are neglected.

Fig. 1 summarizes the disease transmission dynamics of the two strains and Table 1 describes the stratification of the bird population into compartments characterized by the disease and strain-specific status of birds. A susceptible bird can be infected by either the LPAI or the HPAI virus. If infected with the HPAI strain, the bird goes through an asymptomatic phase A_H, when it can die or survive. If it survives, the bird then goes through a symptomatic phase I_H when it can either die with a different probability than that associated with the asymptomatic phase, or recovers, and upon recovery it ends up in the HPAI recovered class R_H. Wood ducks are a species known to be highly susceptible to HPAI as opposed to more famous duck species such as Mallards (e.g. Brown et al., 2006). The one or two birds that recovered after showing mild symptoms in captivity might not survive in the wild. Hence, as a first simplification of the dynamics, we do not include the direct recovery of asymptomatic wood ducks infected by HPAI only. This assumption can be refined in subsequent modeling approaches. Pasick et al. (2007) and Kalthoff et al. (2008) reported that birds shed the virus in both asymptomatic and symptomatic phases, but with the shedding rate lower in the first phase than the second. Hence, we assume that both I_H and A_H classes are infectious, with a reduced infectiousness in the A_H phase. A susceptible bird can also be infected by the LPAI strain, in which case, the bird goes through an asymptomatic phase A_L and eventually recovers and enters into the phase/compartment R_L. The LPAI infection induced death rate is negligible and hence is not incorporated into our model (Pasick et al., 2007). The A_L (LPAI) infected birds shed the LPAI virus (V_L) in the environment at a rate ϕ_L. The cross-immunity effect observed at the individual bird level experimentally is taken into account as described below. A bird recovered from the LPAI strain in the compartment R_L can be infected by the HPAI strain R_L by contact with infectious birds in any of the A_H, I_H, or A_{LH} phases (A_{LH} is to be defined next). If infected, the bird shows symptoms milder than those of fully naive birds (S) infected by HPAI. The A_{LH} compartment consists of asymptomatic birds infected by the HPAI strain due to a preceding LPAI infection that conferred them with *temporary* partial immunity to HPAI. Birds in the A_{LH} compartment have zero HPAI-induced mortality as was observed in Pasick et al. (2007) and Seo and Webster (2001). Note that in their experiment, Pasick et al. (2007) used juvenile birds which are most susceptible to HPAI. Finally, the A_{LH} infected birds can recover and transit into the fully removed compartment R which accounts for birds recovered from both strains or dead. We assume that once a bird has contracted and recovered from HPAI, it remains fully immune to HPAI on the short timescale considered on a migratory stopover.

Recall that Kalthoff et al. (2008) clearly showed that the virus shedding rates changes as HPAI progresses, with the most intense shedding observed in the symptomatic phase. Birds infected with LPAI strains shed the virus in smaller rates compared to asymptomatic naive birds infected by HPAI. As a result, we consider the infection rate to be dependent on the virus shedding intensity, leading to a lower force of infection upon contact with birds in phases A_{LH}, A_H compared to those in I_H. In this model, we use a contact rate which is

Table 1
Definition of the variables and parameters of the two-strain model. Note that, throughout the tables, u.c.w. stands for upon contact with.

S	Birds susceptible to both strains
A_L	Birds infected by LPAI shedding the virus asymptomatically
A_H	Birds infected by HPAI shedding the virus asymptomatically
I_H	Birds infected by HPAI shedding the virus with clinical disease symptoms (very short period in this stage for Mute Swans Kalthoff et al., 2008; Brown et al., 2008)
R_L	Birds recovered from LPAI infection, who have temporarily partial immunity against HPAI. These birds can be infected by HPAI. We assume that the acquired immunity for LPAI is permanent (for the short duration considered here)
R_H	Birds recovered from HPAI
A_{LH}	Birds previously infected by LPAI and are subsequently infected by the HPAI strain. They shed the virus only asymptomatically (due to partial immunity from their LPAI first infection)
R	Removed birds which are either dead or recovered with full immunity to both HPAI and LPAI strains
V_L	LPAI infectious doses in the environment. It is shed by both symptomatic and asymptomatic infected birds
β_A	Infection parameter u.c.w. HPAI asymptomatic carrier
β_I	Infection parameter u.c.w. HPAI symptomatic carrier
β_{LH}	Infection parameter u.c.w. HPAI asymptomatic carrier, who had survived an LPAI infection
μ_{A_H}	Mortality rate of naive asymptomatic birds being infected with HPAI
μ_{I_H}	Mortality rate of naive symptomatic birds being infected with HPAI
γ_H	Rate of transfer from asymptomatic to symptomatic state upon infection by HPAI
α_L	Recovery rate from LPAI infection
α_H	Recovery rate from HPAI infection
α_{LH}	Recovery rate from HPAI infection of those birds who have been previously infected by the LPAI strain and recovered from this strain with partial immunity against the HPAI strain
ω_L	One bird infectious dose (b.i.d.)
ϕ_{A_L}	Rate with which asymptomatic carriers of LPAI produces bird infectious doses
ν_L	Rate of b.i.d. virus decay in the environment (including natural death rate and consumption)
ε_L	Infection parameter u.c.w. one b.i.d. of LPAI virus

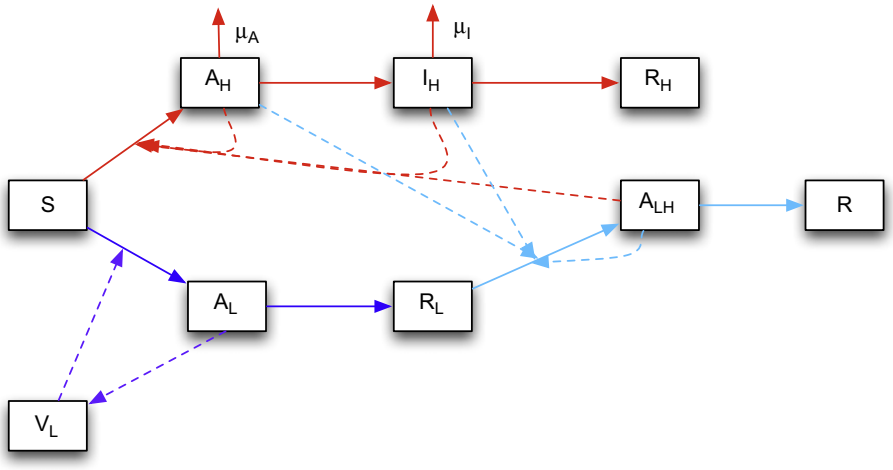

Fig. 1. Flow chart of the two-strain disease dynamics represented by Eq. (1).

independent of the number of birds in the population (standard incidence). In fact, birds are considered to be in direct daily contact only with small numbers of members in their flock during migration and stopovers. Indirect contact with a larger number of birds through the contamination of the environment by LAPI and (in later sections) by HPAI virus is also considered. From the above assumptions and model formulation, the following system of differential equations are used to model the dynamics of the LPAI–HPAI strains. The variables and parameters are detailed in Table 1:

$$\dot{S} = -\varepsilon_L V_L S - (\beta_A A_H + \beta_I I_H + \beta_{LH} A_{LH})S/N,$$

$$\dot{A}_L = \varepsilon_L V_L S - \alpha_L A_L,$$

$$\dot{A}_H = (\beta_A A_H + \beta_I I_H + \beta_{LH} A_{LH})S/N - \mu_{A_H} A_H - \gamma_H A_H,$$

$$\dot{I}_H = \gamma_H A_H - \mu_{I_H} I_H - \alpha_H I_H,$$

$$\dot{R}_L = \underbrace{\alpha_L A_L}_{\text{recovery from LPAI}} \underbrace{-(\beta_A A_H + \beta_I I_H + \beta_{LH} A_{LH})R_L/N}_{\text{2nd infection by HPAI strain}},$$

$$\dot{R}_H = \underbrace{\alpha_H I_H}_{\text{recovery from HPAI}},$$

$$\dot{A}_{LH} = (\beta_A A_H + \beta_I I_H + \beta_{LH} A_{LH})R_L/N - \alpha_{LH} A_{LH},$$

$$\dot{R} = \underbrace{\mu_{A_H} A_H + \mu_{I_H} I_H}_{\text{disease induced death}} + \underbrace{\alpha_{LH} A_{LH}}_{\text{recovery from 2nd HPAI}},$$

$$\dot{V}_L = \phi_{A_L} A_L - \nu_L V_L. \tag{1}$$

3. Reproduction numbers

The model (1) is a system of nine equations with four non-disease compartments (S, R_L, R_H, R), five disease compartments and one virus compartment (A_L, A_H, I_H, A_{LH},V_L). The novelty of the model (1) is to incorporate the viral dynamics of the LPAI strain and the lack of symmetry between the governing equations of the HPAI and LPAI strains, reflecting the clinical observations reported in the literature. In epidemiology, the reproduction number R_0 is defined as the average number of secondary cases of infection upon introduction of one infected individual into a completely susceptible population. It is a threshold parameter. In the absence of backward bifurcation, R_0 less than one implies that an epidemic will die out, while R_0 greater than one implies the spread of the disease. This parameter is useful for characterizing the growth of disease in the early stage of an epidemic, but its significance changes when the disease is no longer restricted to few infected individuals in a large susceptible pool (Brauer et al., 2008; Heffernan et al., 2005). In typical two-strain models, the reproduction number R_0 is usually the largest of the two reproduction numbers associated with the strains examined (Andreasen et al., 1997; Brauer et al., 2008). The reproduction numbers of this system are calculated in Appendix A. Two equilibria are of significance on the time scale considered. One is a disease-free equilibrium in a fully susceptible population $E_0=(S^*,0,0,0,0,0,0,0,0)$, with $S^* = N$ the total number of birds. The other corresponds to a population that has been previously exposed to LPAI, but remains susceptible to HPAI. This equilibrium considered is then $E_1=(S^*,0,0,0,R_L^*,0,0,0,0)$, with $S^*+R_L^* = N$.

Around the equilibrium E_0, the following quantities are found using the next generation matrix approach (see Appendix A):

$$\overline{R}_{0H1} = \frac{S^*/N\beta_I\gamma_H}{(\gamma_H+\mu_{A_H})(\mu_{I_H}+\alpha_H)} + \frac{\beta_A S^*/N}{\gamma_H+\mu_{A_H}}, \quad \overline{R}_{0L1} = \sqrt{\frac{\varepsilon_L S^* \phi_{A_L}}{\nu_L \alpha_L}}, \tag{2}$$

where $\overline{R}_{0H1}$ can be interpreted as the *pseudo*-reproduction number characterizing the spread of the HPAI strain in a population of birds that is fully naive to both HPAI and LPAI infections. The first term accounts for the new HPAI infection generated by an infected bird in its symptomatic infectious stage, while the second term accounts for the new HPAI infection generated by a bird in its asymptomatic infectious stage. Similarly, $\overline{R}_{0L1}$ characterizes the reproduction number for the LPAI strain.

Around the equilibrium E_1, the following quantities are found using the next generation matrix approach (see Appendix A):

$$\overline{R}_{0H2} = \frac{S^*/N\beta_I\gamma_H}{(\gamma_H+\mu_{A_H})(\mu_{I_H}+\alpha_H)} + \frac{\beta_A S^*/N}{(\gamma_H+\mu_{A_H})} + \frac{R_L^*/N\beta_{LH}}{\alpha_{LH}}, \tag{3}$$

$$\overline{R}_{0L2} = \sqrt{\frac{\varepsilon_L S^* \phi_{A_L}}{\nu_L \alpha_L}}, \tag{4}$$

where $\overline{R}_{0H2}$ is interpreted as the analog to the basic reproduction number characterizing the spread of HPAI in a population of birds naive to HPAI only. The introduced infected bird can generate new infections among susceptible S birds as described in the first two terms, or new infections among R_L birds as described in the third term. Similarly, $\overline{R}_{0L2}$ can be interpreted as a pseudo-basic reproduction number in a population of birds naive to HPAI only.

4. Data and epidemiological parameters

The parameters for the disease dynamics of the LPAI and HPAI strains have been gathered from various experimental inoculation studies and previous research papers on the ecology or epidemiology of the LPAI strain in duck populations in the wild. They are summarized in Table 3. The details on the estimation or calculations of these parameters are summarized in the present section.

4.1. LPAI strain, seasonality and migration

The first parameter concerns the amount of LPAI virus needed to cause an infection in a duck. The bird infection dose (b.i.d.) is denoted ω_L. Its value was found to be standard among various studies including the cross-immunization experiment of Pasick et al. (2007) with $\omega_L = 10^6$ EID_{50}. In order to estimate the amount ϕ_{A_L} of b.i.d. shed by one LPAI infected duck per day, we consider the amount of virus per gram of feces excreted multiplied by the amount of gram of feces excreted per day by one infected duck divided by the amount of virus per b.i.d. ω_L. Ducks excrete 7.5–10 kg of feces per year (WHO-EPAR, 2009) and 1 g of their feces contains on average $10^{8.7}$ EID_{50} virions (Webster et al., 1992). Hence, $\phi_{A_L} \approx 10^{8.7} \times 8.75 \times 10^3/(365 \times 10^6) = 2.397 \times 10^{3.7}$ day^{-1}. Note that the average value of 8.75 kg of feces per year was taken for this estimation. Webster et al. (1992) found that ducks shed the AI virus asymptomatically for as long as 2–4 weeks. We take 3 weeks (21 days) to be the average shedding period for LPAI and assume an exponential distribution, leading to $\alpha_L = 1/21$ day^{-1}.

The system of equations for the LPAI subsystem is

$$\dot{S} = -\varepsilon_L V_L S,$$

$$\dot{A}_L = \varepsilon_L V_L S - \alpha_L A_L,$$

$$\dot{R}_L = \alpha_L A_L, \tag{5}$$

$$\dot{V}_L = \phi_{A_L} A_L - \nu_L V_L, \tag{6}$$

with the total constant population $N=R+A_L+S$. Hence, the equation on R_L is redundant. We note that the dynamics governing the amount of virus in the environment V_L is faster than that of the population dynamics. Hence, we can assume that the quantity of virus instantaneously takes the equilibrium value corresponding to the number of A_L in the population at a particular time. If this is

assumed, the above system can be reduced using a fast adjustment of the V_L, i.e. $V_L \approx \phi_{A_L} A_L / v_L$. In order to test this assumption, we display the comparison between the approximation and full solution of Eq. (6) in Fig. 2 for four sets of parameters used in the subsequent study, and we found an excellent match. Consequently, (5) can be reduced to the following sub-system:

$$\dot{S} = -\varepsilon_L(\phi_{A_L} A_L / v_L)S,$$

$$\dot{A}_L = \varepsilon_L(\phi_{A_L} A_L / v_L)S - \alpha_L A_L,$$

$$\dot{R}_L = \alpha_L A_L. \tag{7}$$

From (7) we obtain

$$\frac{dA_L}{dS} = -1 + \frac{\alpha_L v_L}{\varepsilon_L \phi_{A_L} S}, \tag{8}$$

leading to

$$A_L(t) = -S(t) + N + \frac{\alpha_L v_L}{\varepsilon_L \phi_{A_L}} \ln\left(\frac{S}{N}\right). \tag{9}$$

Hence, the controlling parameters of the timing of the peak can be determined analytically and matched to the data collected from the literature. From (7), the peak of the epidemic is reached when

$$\dot{A}_L = 0 \Longrightarrow S_{max} = \frac{v_L \alpha_L}{\varepsilon_L \phi_{A_L}}, \tag{10}$$

with the value of A at the peak of infection given by

$$A_L^{max} = -\frac{v_L \alpha_L}{\varepsilon_L \phi_{A_L}} + N + \frac{v_L \alpha_L}{\varepsilon_L \phi_{A_L}} \ln\left(\frac{v_L \alpha_L}{\varepsilon_L \phi_{A_L} N}\right). \tag{11}$$

Note that the final size equation can also be determined using (9) at $t \to \infty$:

$$S(\infty) - N = \frac{v_L \alpha_L}{\varepsilon_L \phi_{A_L}} \ln\left(\frac{S(\infty)}{N}\right). \tag{12}$$

The key scaling parameter in both (9) and (12) is the same fraction $f = v_L \alpha / (\varepsilon \phi_{A_L})$. Hence, one can either control the peak of the epidemic or the final size population escaping the epidemic. The peak of LPAI prevalence varies from a few percent in the winter season to up to 30% during the weeks preceding the fall migration, particularly when the proportion of juveniles is high and the birds are near water points (e.g. Stallknecht, 1997; Stallknecht and Brown, 2007).

In order to account for the seasonality of LPAI prevalence, here we proceed with setting the key control parameter ratio $f = v_L \alpha / (\varepsilon \phi_{A_L})$ for the LPAI epidemic corresponding to four peaks of A_L 30%, 20%, 10% and 5%. The set R4 corresponds to the highest peak of pre-fall migration season (peak of 30%). The set R1 corresponds to the smallest winter prevalence of 5%. R2 and R3 correspond to prevalences in intermediate seasons, with peaks of 10% and 20%, respectively. Fig. 3 shows the timeseries of the isolated LPAI dynamics for these four sets of parameters (shown in Table 2).

In setting the ratio f, we consider that the water points in which the virus persists are of mid fall temperature around 10 °C. For this temperature, Brown et al. (2009) found that the LPAI virus can survive for an average of 50 days. However, the virus emitted in one location is not expected to stay still at the location of the shedder bird and its flock. If emitted in a water body (which we are considering to be common for wood ducks), diffusion and advection will ensure the dispersal of the virus throughout the fluid body. Assuming otherwise would result in an over-accumulation of virus load in the surrounding of the bird population. This would be equivalent to assuming that the flock is in direct contact with all the virus emitted by the population at all times. This would represent a configuration in which all the birds in the flock considered are constantly swimming in a small closed pond where all the virus is shed and preserved. As a crude abstraction from reality for the purpose of modeling, we account for this dynamic of virus dispersion by assuming that the virus load emitted remain in the surrounding of the shedder location for about 1.14 days, leading to $v_L = 0.875\ \text{day}^{-1}$. Given these parameters, the values of the ratio f lead to a rate of successful LPAI infection upon contact of $\varepsilon_L = 7.42 \times 10^{-9}, 8.85 \times 10^{-9}, 1.19 \times 10^{-8}$, and $1.56 \times 10^{-8}\ \text{day}^{-1}$, corresponding to various seasons of the year.

4.2. HPAI strain and cross-infection parameters

Brown et al. (2006) reported that 2/3 of wood ducks infected with HPAI H5N1 died within 7–8 days. Taking a mean survival of 7.5 days from the first day of sickness leads to $\mu_H = 1/7.5\ \text{day}^{-1}$ (for an exponentially distributed survival). In the same study, the average asymptomatic shedding period was found to be of 5 days. Similarly, we take $\gamma = 1/5\ \text{day}^{-1}$. Wood ducks showed clinical symptoms for 7 days before recovery (for those that recovered). Thus, we take the average duration of HPAI shedding to be the

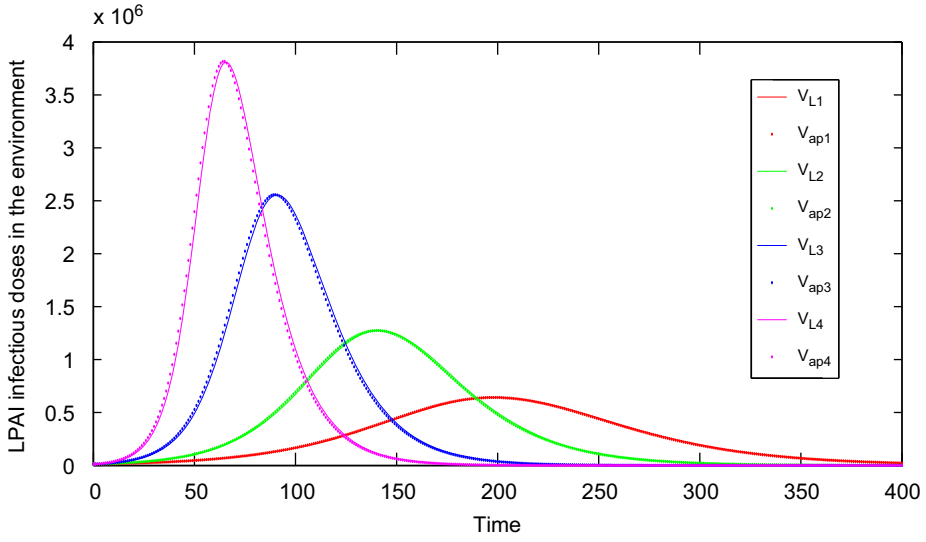

Fig. 2. Comparison between the direct solution of the V_L component of Eq. (6) and its approximate solutions $V_L = \phi_{A_L} A_L / v_L$, assuming a very short time-scale dynamics for the virus in the environment. The four sets of parameters used are those corresponding to the set of parameters R1–R4 detailed in Table 2.

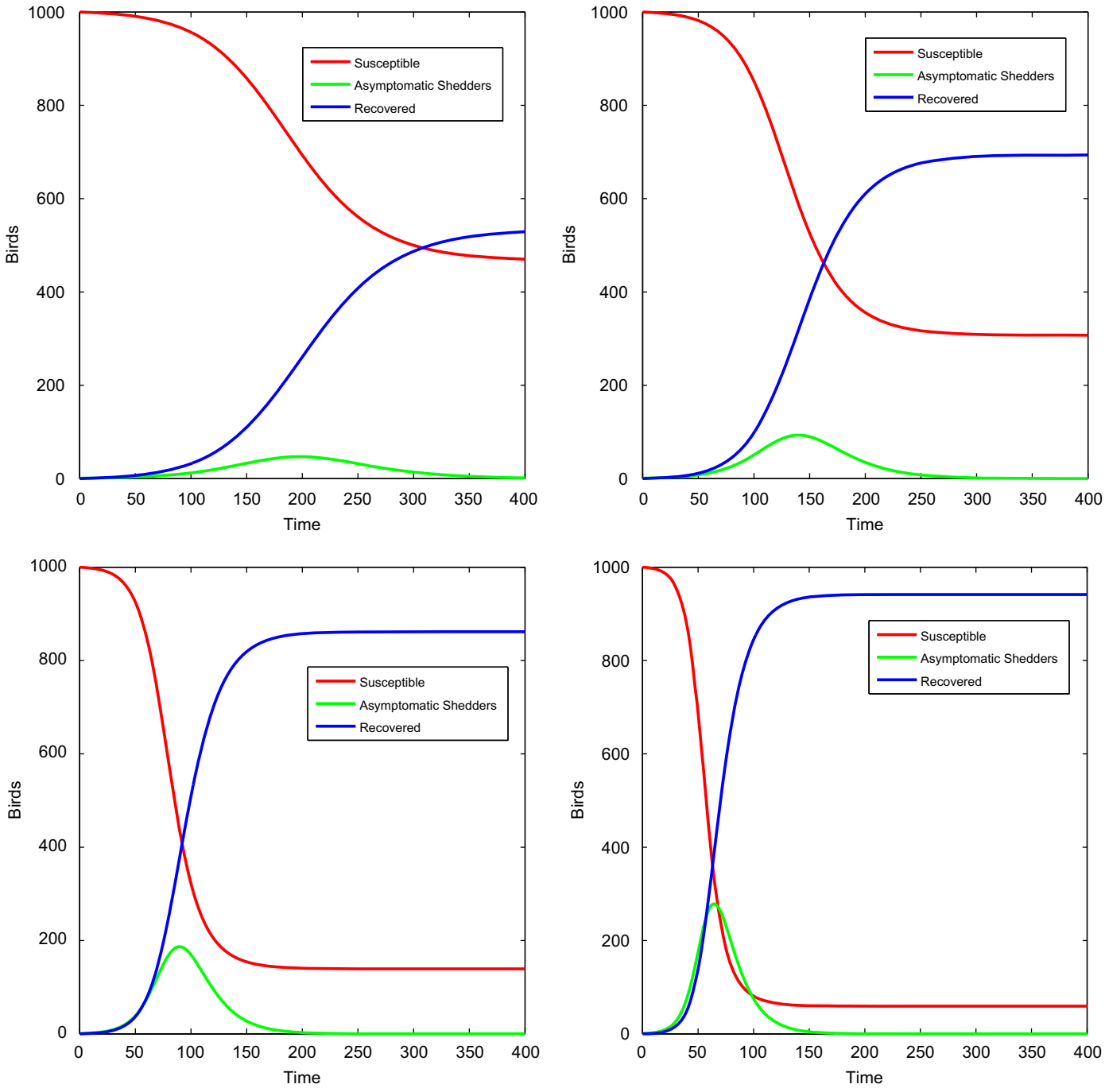

Fig. 3. LAPI disease dynamics with maximum prevalence of A_L^{max}=5%, 10%, 20%, 30% (see parameters R1, R2, R3, and R4 detailed in Table 2 for the full parameter list).

Table 2
Set of parameters for groups of simulations R1–R4, with four values of ε_L, $R_{0L}=\sqrt{\varepsilon_L\phi_{A_L}N/(\nu_L\alpha_L)}$, $\alpha_L=7.14\times10^{-2}$ day^{-1}, $\nu_L=8.75\times10^{-1}$ day^{-1}, $\phi_{A_L}=2.397\times10^{3.7}$ day^{-1}, and the total population $N=1000$.

	ε_L	S_{max}	$S(\infty)$	A_L^{max} (%)	$\overline{R}_{0L1}$
R1	$\varepsilon_{L1}=7.42\times10^{-9}$	700.92	468	5	1.19
R2	$\varepsilon_{L2}=8.85\times10^{-9}$	587.54	308	10	1.30
R3	$\varepsilon_{L3}=1.19\times10^{-8}$	434.46	141	20	1.51
R4	$\varepsilon_{L4}=1.56\times10^{-8}$	333.72	60	30	1.73

inverse of $\alpha_H=1/7$ day^{-1}. According to Kalthoff et al. (2008), the birds infected by LPAI prior to the HPAI infection shed the virus principally oropharyngeally for 3 days (asymptomatically), then recover. We thus take the average duration of shedding of pre-LPAI infected birds to be the inverse of $\alpha_{LH}=1/3$ day^{-1}.

In (1), the infection parameter β_{I_H} is the product of the number of contacts c between an infectious and susceptible bird per unit time and p the probability of successful infection upon such contact. That is, $\beta_{I_H}=c\times p$. The average number of daily close contacts for a bird within a flock is taken to be 10. We take a range of values for the transmission probability p of 0.03975–0.80. We

Table 3
List of parameter values and sources used.

ω_L	10^6 EID_{50}	Pasick et al. (2007) with H5N2
ϕ_{A_L}	$2.397\times10^{3.7}$ day^{-1}	Webster et al. (1992) and WHO-EPAR (2009)
ε_L	from 7.42×10^{-9} to 1.56×10^{-8} day^{-1}	
ν_L	8.75×10^{-1} day^{-1}	Brown et al. (2008)
α_L	4.76×10^{-2} day^{-1}	Webster et al. (1992)
β_{I_H}	1.5–3.0 day^{-1}	Brown et al. (2006) and Kalthoff et al. (2008)
β_{A_H}	$\beta_{I_H}/1.75$ day^{-1}	Brown et al. (2006) and Kalthoff et al. (2008)
γ_H	2.0×10^{-1} day^{-1}	Brown et al. (2006)
α_H	1.43×10^{-1} day^{-1}	Brown et al. (2006)
μ_H	1.33×10^{-1} day^{-1}	Brown et al. (2006)
β_{LH}	$\beta_{IH}/2.0$ day^{-1}	Kalthoff et al. (2008)
α_{LH}	3.33×10^{-1} day^{-1}	Kalthoff et al. (2008)

selected four values displayed in Fig. 4: $p_1=0.03975$, $p_3=0.0443$, $p_5=0.05$, and $p_6=0.1$. These lead to HPAI isolated dynamics with peak infectious populations of about 7.44%, 10.8%, 15%, and 53% with $A_H^{max}=$ 43.63, 63.64, 89.4, 350 and $I_H^{max}=$ 30.74, 44.35, 60.83, 185, respectively. Finally, according to Kalthoff et al. (2008) (Fig. 1D), the shedding rate during the symptomatic phase is 1.75 times as intense as the shedding rate during the asymptomatic phase of the disease. In addition, the shedding rate during the HPAI symptomatic phase is found to be twice as intense as the shedding during the asymptomatic phase of the partially immunized birds previously infected by LPAI. Hence, we choose $\beta_{A_H}=\beta_{I_H}/1.75$ and $\beta_{LH}=\beta_{I_H}/2$.

5. Simulation and results

5.1. Effect of LPAI on the onset and dynamics of HPAI

Here we focus on 16 sets of parameters. Four LPAI specific sets of parameters (R1–R4) correspond to a change of seasonality faced by the birds during their migration (see Section 4.1). The four HPAI specific sets of parameters correspond to case scenarios of HPAI in the range of data reported in the literature. The four cases correspond to probabilities of infection upon contact with transmission probabilities p_1, p_3, p_5, and p_6 corresponding to HPAI pseudo-reproduction numbers of $\overline{R}_{0H1}\approx1.55$,1.7,1.8, and 3.9, respectively. Throughout this section, the initial population is assumed not to be previously exposed to either LPAI or HPAI strains.

Figs. 5 and 6 show the timeseries of the number of birds in all disease stages for the full dynamics with both HPAI and LPAI strains co-circulating and modeled by (1). Clearly, the relative values of LPAI and HPAI control parameters lead to roughly three types of configurations. The first regime is that in which the HPAI strain dominates and the increase of prevalence of LPAI from one season to the next does not significantly influence the HPAI death toll. The death toll remains higher than 40% (Fig. 5), reaching up to 70% in the extreme case scenario of HPAI probability of transmission $p_6=0.1$ (two bottom rows of Figs. 5 and 6). In this first regime, the LPAI strain remain too slow to compete and spread. Its pseudo-reproduction number associated with LPAI $\overline{R}_{L01}$ is smaller than that associated with HPAI $\overline{R}_{0H1}$, with $\overline{R}_{0H1}-\overline{R}_{0L1}\gtrsim O(10^{-1})$ (all panels in Fig. 5). In the second regime in which $\overline{R}_{0H1}$ and $\overline{R}_{0L1}$ are almost equal ($O(10^{-1})\gtrsim|\overline{R}_{0H1}-\overline{R}_{0L1}|$), the influence of LPAI is significant in reducing the number of birds infected by HPAI. As a result, the overall death toll of HPAI is reduced. From the comparison of the results in Fig. 6 we note that the main difference between cases with $\overline{R}_{0L1}\gtrapprox\overline{R}_{0H1}$ and $\overline{R}_{0L1}\lessapprox\overline{R}_{0H1}$ is the final number of LPAI recovered birds and as a result, the final number of birds escaping both LPAI and HPAI. This can be seen, for example, for the two cases in which ($\overline{R}_{L01}=1.51$,$\overline{R}_{H01}=1.55$) and ($\overline{R}_{L01}=1.73$,$\overline{R}_{H01}=1.7$) (row 1 left and row 2 right).

The last regime illustrated by Fig. 6 (row 1 right) is that in which the pseudo-reproduction number of the LPAI strain is larger than that of HPAI with $\overline{R}_{0L1}-\overline{R}_{0H1}>O(10^{-1})$. In this regime, the LPAI dynamics is sufficiently rapid to hinder the initiation of the epidemic of HPAI. A considerable reduction in the number of HPAI dead and recovered birds can be observed. These are as low as $\approx$195 and 100, respectively.

In sum, the co-circulating LPAI and HPAI strains in a naive population can lead to a reduction of HPAI induced death at the population level. In particular, the increase of the prevalence of LPAI (as ε_L increases) with seasonality affects more significantly the final number of dead birds compared to its effect in reducing the final number of HPAI recovered groups. In turn, we can see that the outcome of the HPAI epidemic is highly dependent on the season in which the HPAI strain is introduced into the population. Moreover, it could be under-detected in the wild in post-LPAI peak season, which is usually in the Fall.

5.2. Mitigation of HPAI epidemic in non-LPAI-naive population

Recall that during the 1997 Hong Kong outbreak among poultry, an LPAI strain was suspected to be circulating and to have been present prior to the onset of HPAI. A preceding circulation of LPAI would also be the most likely scenario in populations of wild birds such as wood ducks or geese in which LPAI is very common. We ignore the mechanisms leading to the introduction of HPAI on such a population, and consider the case where HPAI is introduced in a wood duck population with a range of LPAI recovered birds arising from a precedent LPAI epidemic. We consider a range of initial conditions in which the proportion of susceptible $S(0)$ and LPAI recovered $R_L(0)$ varies, and $S(0)+R_L(0)=N=$ constant. Depending on the time of year and delay between the LPAI and HPAI epidemics, a range of LPAI recovered birds present at the onset of HPAI ($R_L(0)$) is examined.

Figs. 7 and 8 show the final values of S, D, R_L, R_H and R as a function of the initial number of LPAI recovered birds from preceding LPAI epidemic $R_L(0)$. The results obtained for a fully naive population (discussed in Figs. 5 and 6) correspond to the points $R_L(0)=0$. Most graphs show a decrease of final death $D(\infty)$ and HPAI recovered birds $R_H(\infty)$ with the increase of initial LPAI recovered birds $R_L(0)$. The rate of decay of the final HPAI induced death $D(\infty)$ is always found to be larger than that of the final HPAI recovered birds $R_H(\infty)$. For a fixed $\overline{R}_{0H1}$, the increase of $\overline{R}_{0L1}$ (rows from left to right) leads to smaller values of $D(\infty)$ and $R_H(\infty)$. However, in the extreme case where $\overline{R}_{0H1}\gg\overline{R}_{0L1}$ (bottom panels), the increase of the transmission parameters of a LPAI no longer affects the epidemic of HPAI. This was already observed in the case of fully naive population discussed in the previous section. However, the change in the initial number of LPAI recovered birds $R_L(0)$ due to a preceding LPAI epidemic remains significant in inducing a rapid decrease of the final HPAI dead and recovered birds, even in the extreme case of dominant HPAI strain (e.g. $\overline{R}_{0H2}=3.9$). The effect of prior LPAI epidemic on HPAI observed can only be partially rationalized by the reduction of the initial pools of susceptible $S(0)$ as $R_L(0)$ increases. In fact, if the curve of $R_L(\infty)$ is below the diagonal, the HPAI strain is efficient enough to infect both pools of susceptible and LPAI recovered, and hinders the spread of co-circulating LPAI. Then, the number of fully recovered $R(\infty)$ and susceptible $S(\infty)$ birds have a non-monotonic dependence on $R_L(0)$ and change considerably from one set of parameters to the next. In all cases considered, except for the HPAI dominant $\overline{R}_{0H1}=3.9$ (bottom rows), we observe an initial phase of increase of the final number of susceptible $S(\infty)$ escaping the epidemic as $R_L(0)$ increases.

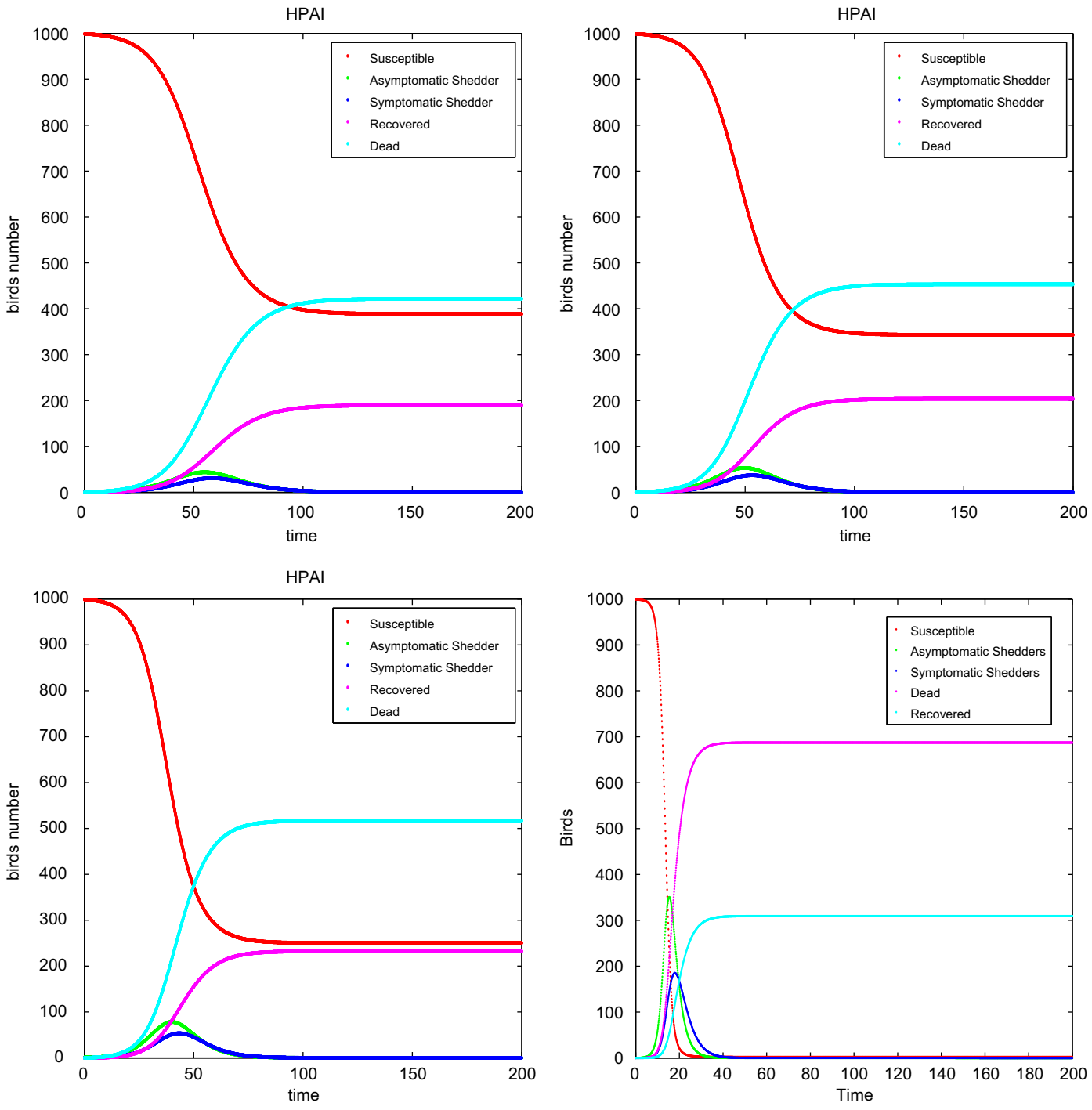

Fig. 4. H5N1 disease dynamics with $c = 10\ \text{day}^{-1}$ and transmission probabilities, (top left) $p_1 = 0.03975$, (top right) $p_3 = 0.0443$, (bottom left) $p_5 = 0.05$, and (bottom right) $p_6 = 0.1$, corresponding to peaks in the HPAI infectious population of about 7.44%, 10.8%, 15%, and 53% with $A_H^{max} = 43.63, 63.64, 89.4, 350$ and $I_H^{max} = 30.74, 44.35, 60.83, 185$, respectively.

Beyond a threshold value of $R_L(0)$, a second phase of decrease of $S(\infty)$ is initiated. The same general trend can be observed for the HPAI–LPAI recovered population $R(\infty)$. The pseudo-reproduction numbers of the two strains in isolation $\overline{R}_{0H1}$ and $\overline{R}_{0L1}$ are not adequate to provide explanation of the trends of the final size quantities observed in Figs. 7 and 8.

To complete this discussion, we now describe the change of $\overline{R}_{0H2}$ (3) and $\overline{R}_{0L2}$ (4).

Fig. 9 (top left) shows the HPAI quantity $\overline{R}_{0H2}$ with $p = p_1$ and that of four groups of $\overline{R}_{0L2}$ corresponding to the change of prevalence of LPAI from ε_1 in Fig. 7 (top left) to ε_4 in Fig. 8 (top right). Both $\overline{R}_{0H2}$ and $\overline{R}_{0L2}$ decrease with the increase of initial LPAI recovered $R_L(0)$. Beyond threshold values of $\overline{R}_{0H2} = 1$ and $\overline{R}_{0L2} = 1$ we observed a transition to a regime in which the final and initial numbers of LPAI recovered birds become equal $R_L(\infty) = R_L(0)$ (or equivalently $S(\infty) = N - R_L(0)$). In this regime, the spread of both strains is hindered. Moreover, when comparing Fig. 9 (top left) and Fig. 8 (top right) the changes of trend preceding the local maximum of $S(\infty)$ and local minimum of $R_L(\infty)$ are due to a transition of regime from $\overline{R}_{0H2} > 1$ to $\overline{R}_{0H2} < 1$ (occurring at $R_L(0) \approx 575$). Beyond this transition, $S(\infty)$ decreases; however, this is no longer due to the disease dynamics, but is instead due to the decrease of $S(0)$

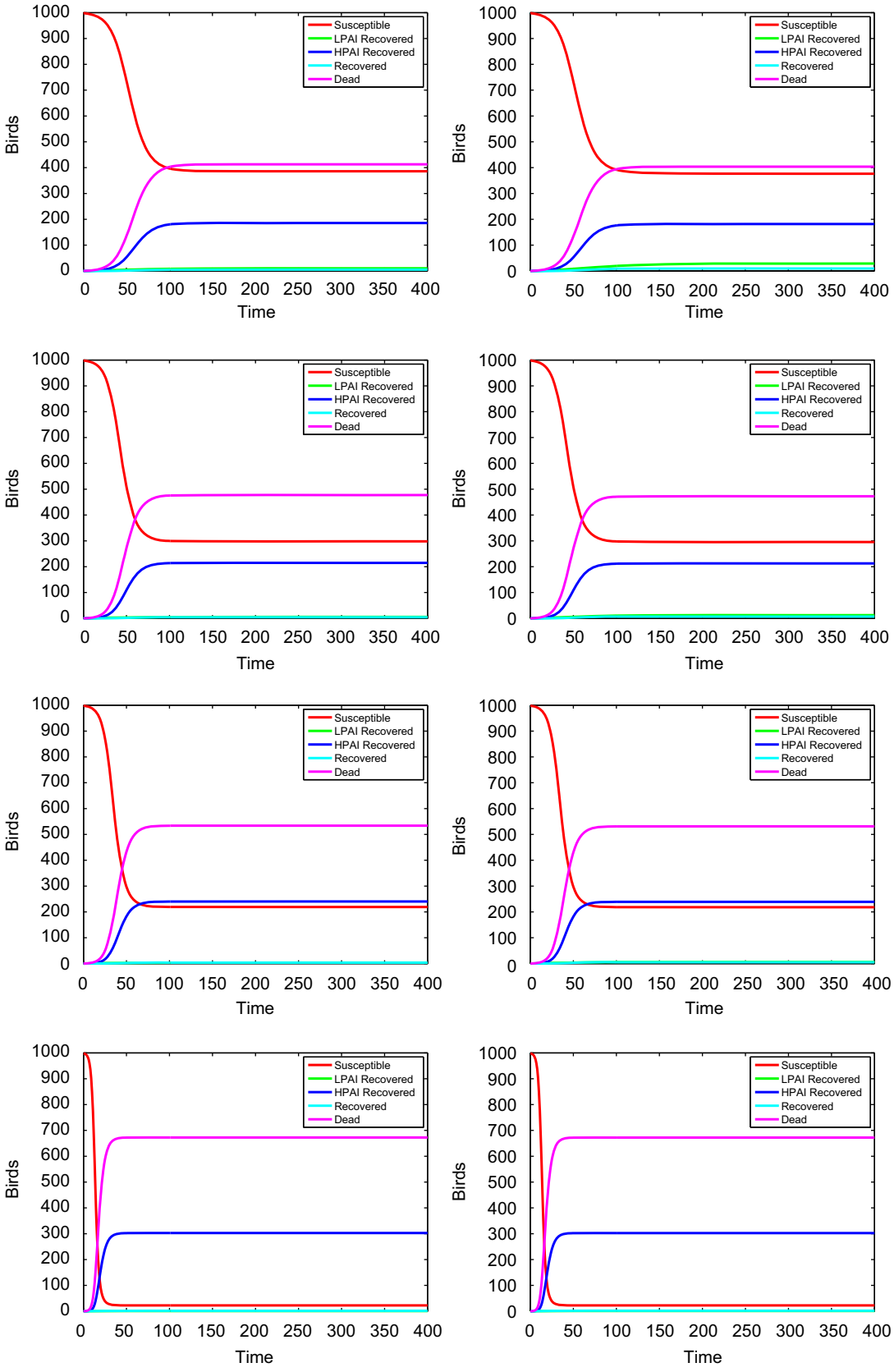

Fig. 5. Full simulation timeseries with $R_L(0)=0$ and starting from one HPAI and one LPAI infected bird with HPAI parameter values of (top row) $p_1 = 0.03975$, (second row) $p_3=0.0443$, (third row) $p_5=0.05$, and (fourth row) $p_6= 0.1$, and LPAI parameter sets (left panel) R1 and (right panel) R2.

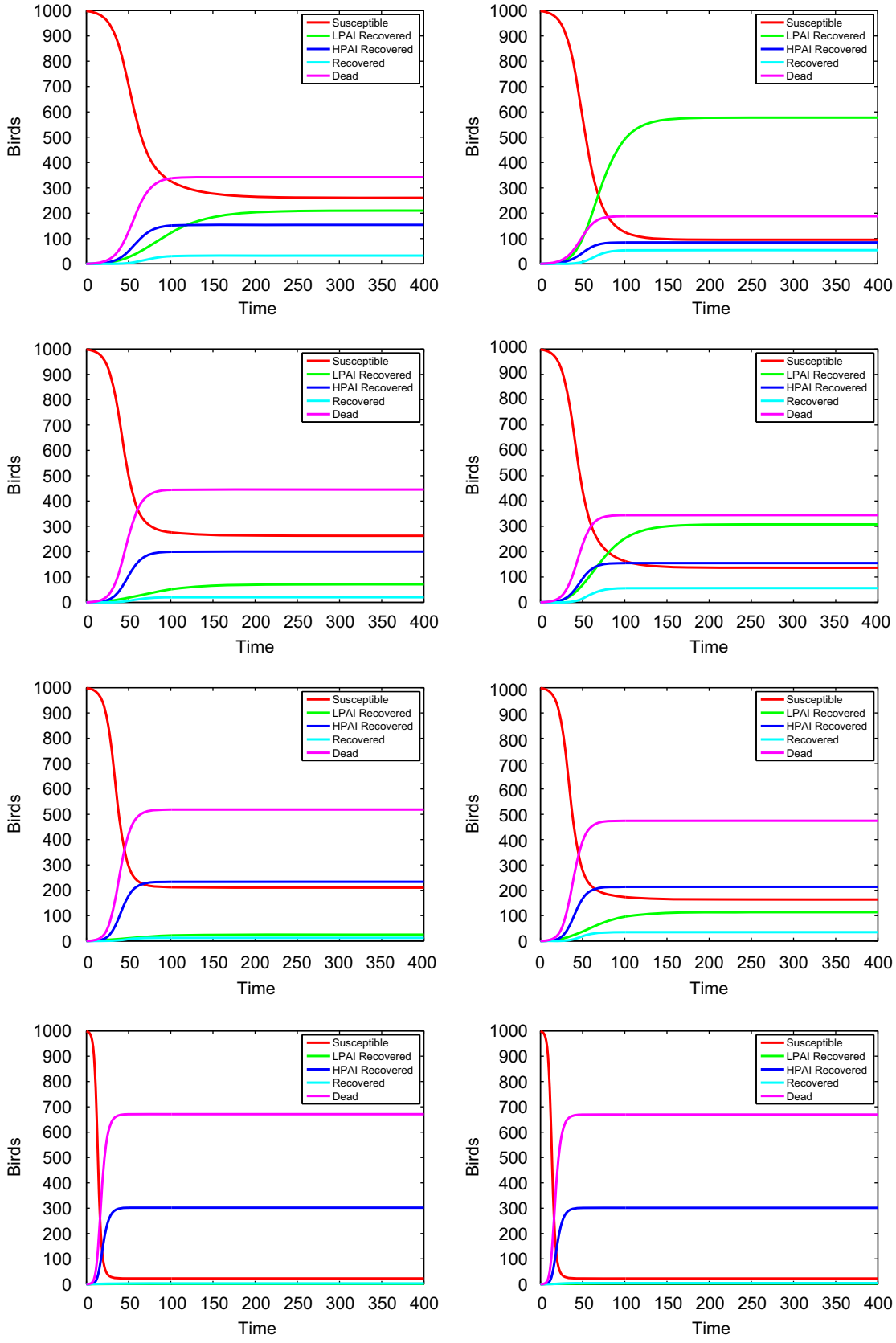

Fig. 6. Full simulation timeseries with $R_L(0)=0$ and starting from one HPAI and one LPAI infected bird with HPAI parameter values of (top row) $p_1 = 0.03975$, (second row) $p_3=0.0443$, (third row) $p_5=0.05$, and (fourth row) $p_6= 0.1$, and LPAI parameter sets (left panel) R3 and (right panel) R4.

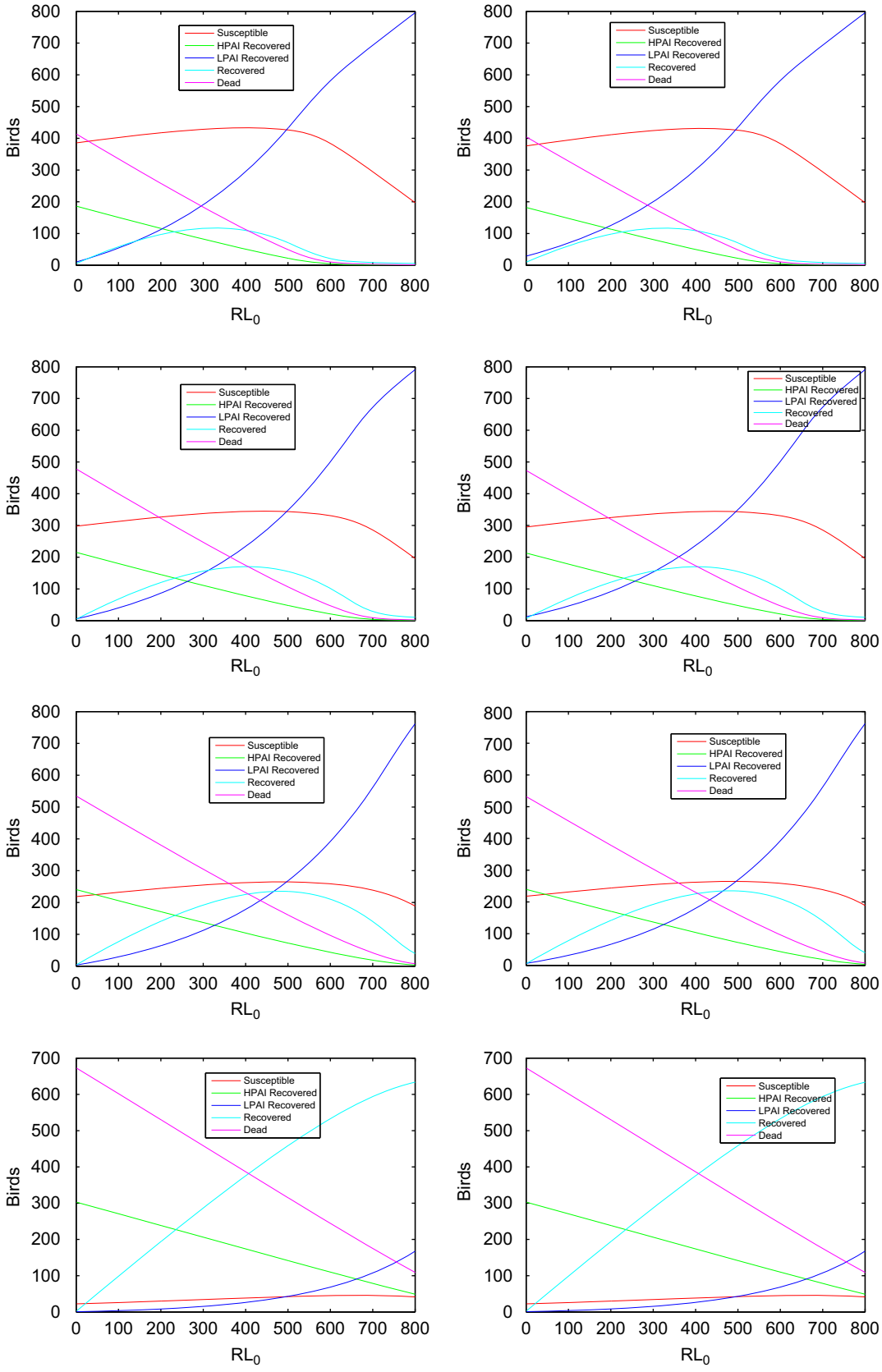

Fig. 7. Full simulation of equilibria (time $t=400$) as a function of the initial amount of LPAI recovered for HPAI (top row) $p_1 = 0.03975$, (second row) $p_3=0.0443$, (third row) $p_5=0.05$, and (fourth row) $p_6= 0.1$, and for LPAI (left panel) $\varepsilon_L = \varepsilon_1$ and (right panel) $\varepsilon_L = \varepsilon_2$.

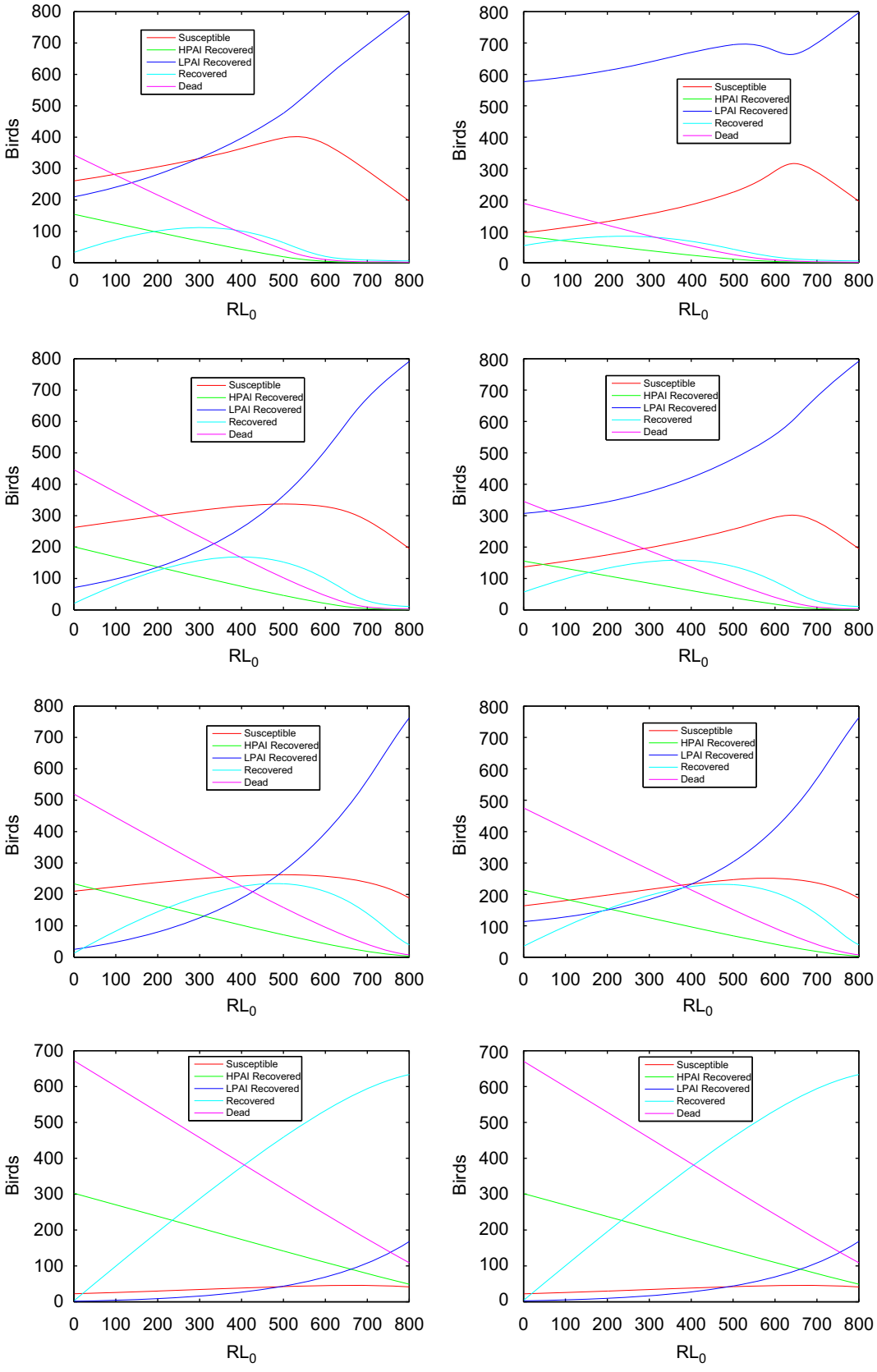

Fig. 8. Full simulation of equilibria (time $t=400$) as a function of the initial amount of LPAI recovered for HPAI (top row) $p_1=0.03975$, (second row) $p_3=0.0443$, (third row) $p_5=0.05$, and (fourth row) $p_6=0.1$, and for LPAI (left panel) $\varepsilon_L=\varepsilon_3$ and (right panel) $\varepsilon_L=\varepsilon_4$.

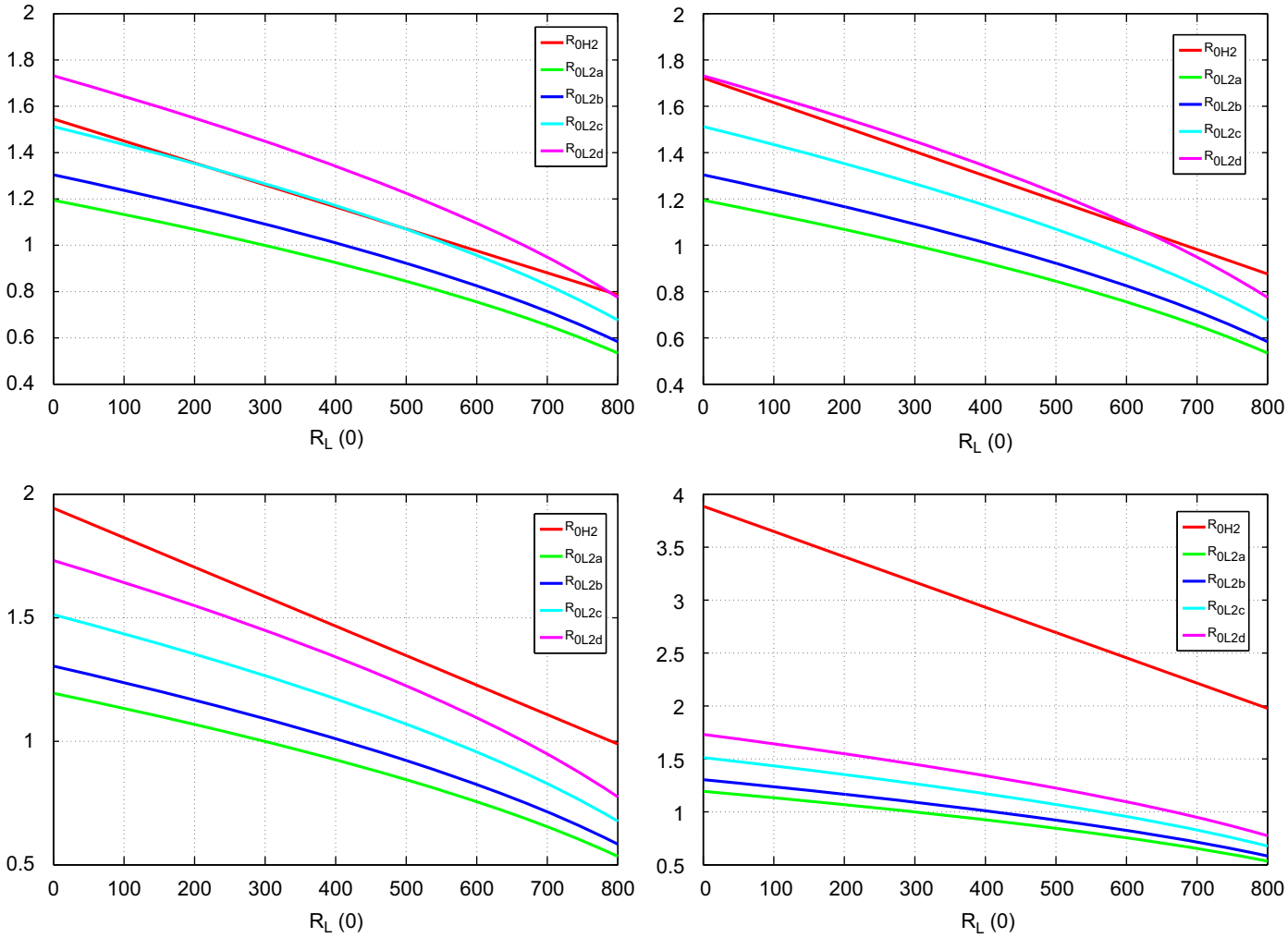

Fig. 9. Comparison of the values of $\overline{R}_{0H2}$ and $\overline{R}_{0L2}$ corresponding to the HPAI parameters (top left) p_1, (top right) p_3, (bottom left) p_5, and (bottom right) p_6 and LPAI parameters ε_{L1},ε_{L2},ε_{L3},ε_{L4} used in Figs. 7 and 8 as a function of the initial LPAI recovered population $R_L(0)$. Note that R_{0L2a} corresponds to the LPAI parameter ε_{L1}, R_{0L2b} corresponds to the LPAI parameter ε_{L2}, etc.

associated with the increase of $R_L(0)$. Other transitions characterized by change of regime at $\overline{R}_{0H2}=1$ can also be observed in other panels, e.g. at $R_L(0)$=700 for $p=p_3$ (Fig. 9 top right) or $R_L(0)$=800 for $p=p_5$ (Fig. 9 bottom left). In the last panel (bottom right), $\overline{R}_{0H2}\gg 1$ for all values of $R_L(0)$ and it is associated with a distinct dynamic in which $R(\infty)$ increases for all values of $R_L(0)$ (lower panels of Figs. 7 and 8). In sum, a threshold value of one can be crossed by $\overline{R}_{0H2}$, $\overline{R}_{0L2}$ as $R_L(0)$ increases. However, as long as one of the two remains larger than one, no significant changes in the final state are observed in the two-strain system. What emerges is that the effect of a pre-epidemic of LPAI for the mitigation of the deadly impact of HPAI is stronger than that of a co-circulating LPAI strain. We further examine this statement in what follows.

Consider the ratio $r=(S+R_L)(\infty)/(S+R_L)(0)$ as a function of $R_L(0)$. $r=1$ if no bird goes through the HPAI epidemic and $r<1$ otherwise. Hence, r allows for a more direct quantification of the mitigating effect of both *preceding* and *simultaneous* LPAI epidemics on the invasion or spread of HPAI. In Fig. 10, each graph corresponds to a different HPAI parameter (p_1,p_3,p_5 and p_6). On each graph, a co-circulating and preceding LPAI is examined for the four (R1–R4) LPAI sets of parameters. We can see that the increase in ε_i leads to higher values of r. For a fall prevalence of LPAI (ε_4) and $p=p_1$ (top left), the total population escaping HPAI increases from 67% to 90% as $R_L(0)$ increases from 0 to 50%. For a smaller LPAI prevalence (e.g. ε_3), the change is from about 48% to 85% for the same increment of $R_L(0)$ (same figure). The impact of LPAI transmission parameters is particularly noticeable for small values of $R_L(0)$ (e.g. below $\approx 40\%$) above which all curves tend to collapse. In addition, the effect of LPAI transmission parameters decreases as p_i increases, e.g. at $R_L(0)=50\%$ the difference between the number of birds escaping HPAI for the co-circulating LPAI with ε_4 and another LPAI epidemic with ε_3 varies from $\approx 10\%$ to 2% to 0% as p increases from p_1 (top left) to p_3 (top right) to p_5 (bottom left). In conclusion, the impact of the change of season decreases from one figure to the next as the collapse of the four R1–R4 curves shows; however, despite the increase of $\overline{R}_{0H2}$, which becomes larger than $\overline{R}_{0L2}$ (Fig. 9), the effect of the preceding epidemic ($R_L(0)$) remains the most important factor in the increase of the number of birds escaping HPAI all together. This conclusion is not altered when we modify the constant population assumption and consider the case where dead birds are separated from fully recovered birds. For example, in the case of constant population considered herein, r increases from 28% to 50% as $R_L(0)$ increases from zero to 50% even in the case where $\overline{R}_{0H2}$ is larger than one and larger than all values of $\overline{R}_{0L2}$ (bottom left figure). In the case of non-constant population N, where dead birds are distinct from fully recovered birds, our simulations (not shown here) show that the effect of the preceding epidemic is even more important with, for example, a rise of r from 8.8% to 44% for the same parameters and increments of $R_L(0)$.

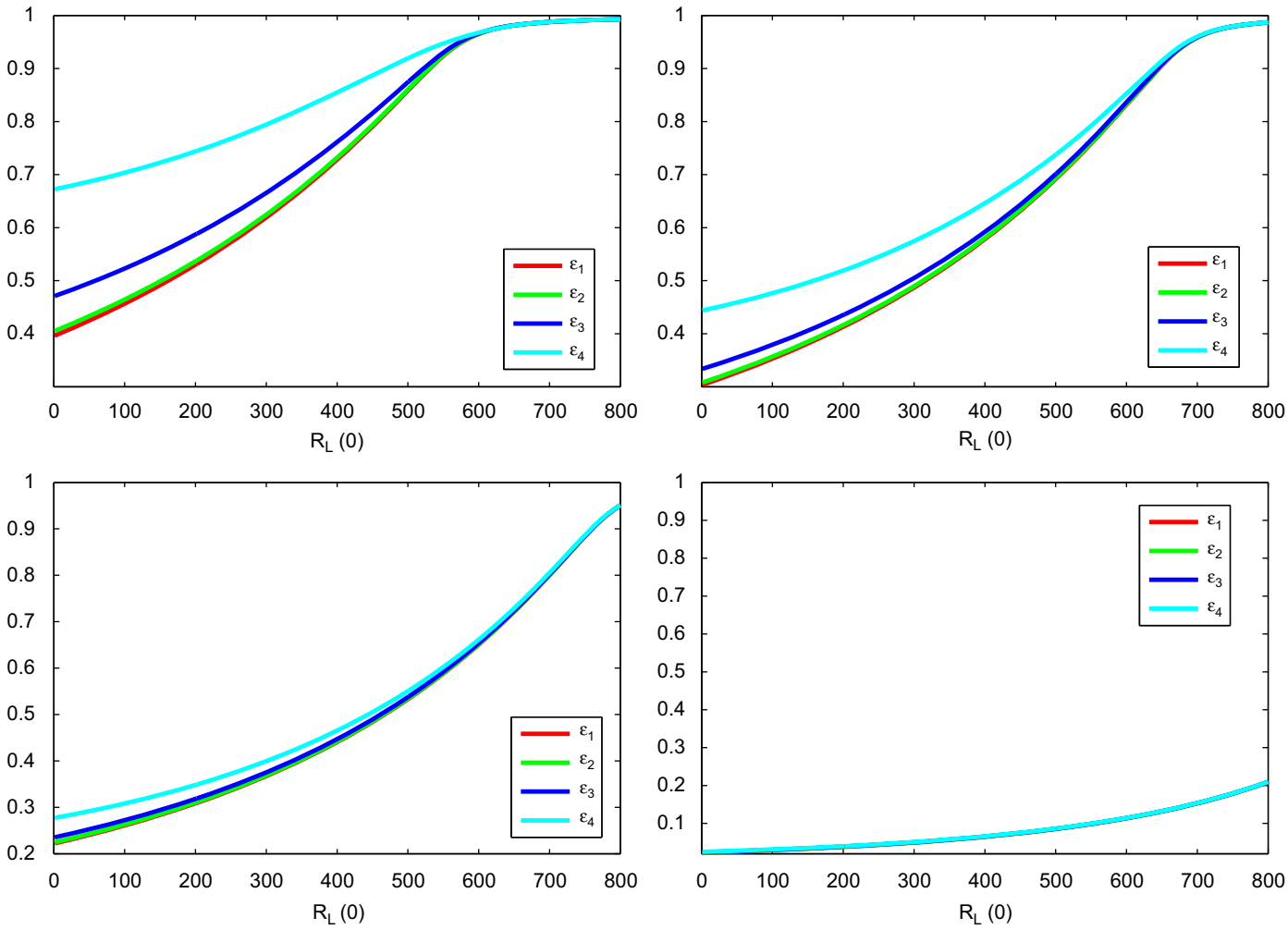

Fig. 10. Ratio of final over initial number of birds in compartments S and R_L, $(S+R_L)(\infty)/(S+R_L)(0)$ as a function of $R_L(0)$ and for HPAI transmission probabilities of (top left) p_1, (top right) p_3, (bottom left) p_5, and (bottom right) p_6 and with four prevalences of LPAI characterized by transmission parameters $\varepsilon_L=\varepsilon_1,\varepsilon_2,\varepsilon_3,\varepsilon_4$. This ratio quantifies the number of birds escaping the HPAI strain epidemic.

6. Discussions and conclusions

The spread of HPAI H5N1 remains a threat for both wild and domestic bird populations. Low pathogenic strains of avian influenza were reported to induce partial immunity to HPAI in poultry and some wild birds inoculated with both strains. Based on the reported data and experiments, we examined the extent to which this partial immunity observed at the individual bird level would affect the outcome of outbreaks among migratory bird populations in the wild. Various periods of the year were examined taking into account the change in seasonal prevalence of LPAI in wild bird populations. In light of the systematic observations of a higher oropharyngeal shedding for the HPAI strain in the literature, we have focused on the dominant role of environmental indirect transmission of LPAI and the direct transmission of HPAI. We found a distinct mitigating effect of LPAI on the death toll induced by the HPAI strain. This effect is particularly important for non-LPAI-naive population of birds which were previously infected by LPAI. It is important to highlight that this effect would take place if the gap between an LPAI and HPAI outbreak would be in the range of up to a few months only. In particular, for a given particular HPAI virus the seasonal change in the prevalence of LPAI could reduce the population infected by HPAI from 60% to 30% (Fig. 10). This effect increases as the gap between the end of the LPAI and the onset of the HPAI epidemic decreases. This mitigating effect decreases with the virulence of HPAI.

The importance of environmental indirect transmission of LPAI due to a dominant cloacal virus shedding is commonly accepted in the literature; however, the role of this route of transmission of HPAI remains unclear. In fact, although oropharyngeal shedding is dominant, cloacal shedding of HPAI strain remains non-zero. Hence, in this final section we discuss the effect of an additional environmental indirect HPAI transmission. The modified flow chart summarizing the dynamics is presented in Fig. 11, which describes the model displayed in Appendix B.

Starting from an initial state for which a residual infection dose of HPAI virus is present in the environment, with no trace of LPAI virus in the environment and no infectious birds, we examine the dynamics of an HPAI epidemic where the only mode of transmission is the indirect fecal-to-oral route (or environmental route). Fig. 12 shows the dynamics obtained for various forces of infection and associated prevalences. Recall that avian influenza prevalence depends on the geographical location of the birds during migration, which is associated to particular times of the year. The values for the environmental HPAI transmission parameter ε_H in equations of Appendix B.1 are taken to be $\varepsilon_H=2.3,2.95,3.5,4.1,6.45\times10^{-10}$ day^{-1}. These correspond to peaks of asymptomatic HPAI shedders of 1%,4%,7%,10%,20%, respectively. The detailed estimation of the parameters for this model is given in Appendix B.

Consider first the HPAI epidemic dynamics when the effect of the environment indirect transmission mechanism is introduced.

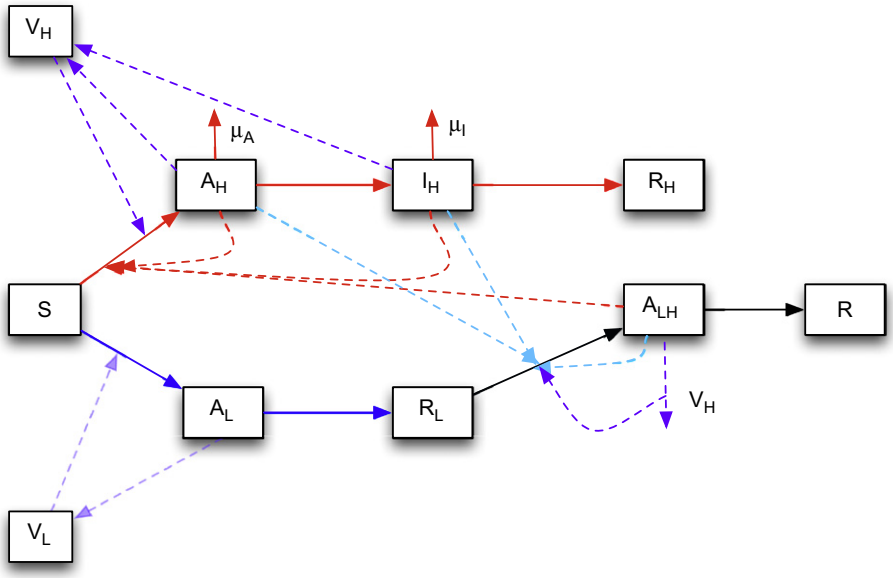

Fig. 11. Flow chart of the two-strain disease dynamics with environmental transmission for both strains.

In order to do so, we compare four cases of HPAI transmission with the following characteristics. All four cases are set to achieve a peak of I_H+A_H of 9% in four different modes of transmission (Table 4). In Case 1, the HPAI epidemic is only due to contact based direct transmission and no environmental shedding. In Case 2, the HPAI transmission is based on both contact and environmental indirect transmission; however, the contact is the predominant transmission mechanism. In Case 3, the HPAI epidemic is only due to indirect environmental transmission with no direct contact. Finally, in Case 4 both direct and indirect transmission mechanisms are present; however, the indirect environmental mechanism is predominant. All four cases were initiated with one infected bird in a fully susceptible population and a virus-free environment. Fig. 13 shows the timeseries of S, R_H, D, A_H + I_H, and V_H for Cases 1, 2, 3, and 4 where only the HPAI strain is present.

This hypothetical comparison, using the available data in the literature to parametrize the model, shows that for the same peak in the population of infectious HPAI birds, the dynamics dominated by contact transmission (cases 1 and 2) lead to a lower mortality than the cases dominated by environmental indirect transmission of HPAI. The difference is not huge, but it is nevertheless to be noted given that we chose the peak of infections to be identical in the four cases. Hence, this disparity calls for a further examination of the epidemic data in the wild as one would possibly expect a larger death toll in epidemics dominated by environmental transmission (for example around small and slow water points). Note that when considering the effect of indirect environmental transmission of HPAI, the epidemic was initiated by one infected bird rather than an infectious dose. We observed that the initiation of the epidemic by an infectious dose produces a similar dynamic and final size values for each compartment; however, the onset of the epidemic is slower. This underlines the fact that onset of epidemics due to residual environmental contamination could take some time and would be plausible only in areas where the birds would reside for long times (e.g. wintering grounds, the summer grounds, and long stopovers along migratory routes).

Finally, adding the co-circulating LPAI virus in the environment to the above four cases leads to the dynamics described in Fig. 14. As expected, the introduction and the increase in its indirect environmental transmission parameter (ε_L) leads to a mitigating effect reducing the overall death toll of HPAI. In addition, we observe that seasonality (change in ε_L) more significantly affects the outcome of the HPAI epidemics that are dominated by indirect environmental contamination.

To summarize, we find that HPAI outbreaks would lead to higher death tolls when dominated by indirect environmental transmission rather than contact direct transmission for the available data and information reported. When indirect transmission is dominant, the transmission mechanisms can be seen as being a two step mechanism with one bird-to-environment segment; and a second environment-to-bird segment. Intuitively, this can be expected to lead to a delay and extension of the "effective" infectious period compared to the mean infective period of direct bird-to-bird transmission. In our simulations, we observe that the combination of these two phases lead to a small delay in the onset of the epidemic, but we also observe a slight extension of the epidemic (e.g. Fig. 13 bottom panels where direct transmission is compared to indirect transmission). This can be explained by the persistence of the virus in the environment leading to new infections generated for a bit longer than what is observed in a contact dominated setting. Moreover, as the season of introduction of HPAI changes, the LPAI mitigating effect on the death toll of HPAI is observed to be more significant for HPAI epidemics dominated by environmental indirect transmission. As seen in Fig. 13 and discussed previously, an HPAI epidemic dominated by indirect transmission leads to a delay in the onset of HPAI. It appears that this delay or slow-down of the HPAI epidemic take off gives a greater advantage to the LPAI strain leading to a higher mitigating effect of the death toll. The delay of onset of HPAI allows for a greater proportion of susceptible birds to be infected by LPAI first. These birds escape a fate of death if subsequently infected by the HPAI strain. The pool of susceptibles to be directly infected by HPAI is thus reduced.

Finally, the mitigating impact of a previous LPAI infection on the mortality and prevalence of a HPAI outbreak should be interpreted with caution. In fact, the partial immunity leads to the extension of the H5N1 asymptomatic infection stage during which shedding of the virus continues to occur. As a result, infected asymptomatic wild birds could be allowed to shed the virus over longer distances due to a pre-infection with a LPAI strain.

The infected birds would not show detectable symptoms early on, which could delay the detection of the environmental contamination by the virus. This time lag in detection could result in a

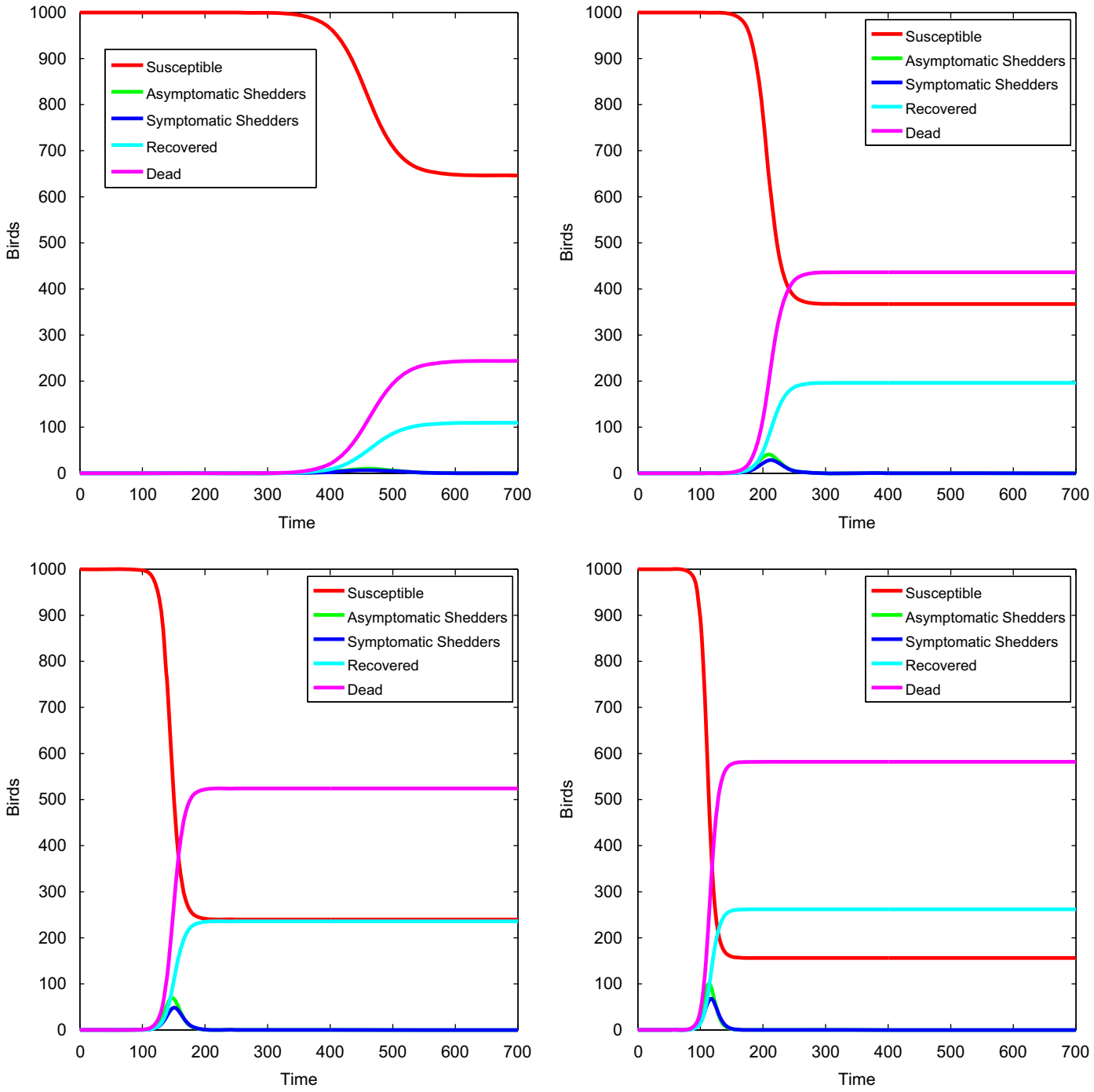

Fig. 12. The environmental transmission parameter for the HPAI is set to be $\varepsilon_H = 2.3, 2.95, 3.5, 4.1, 6.45 \times 10^{-10}$ day^{-1} corresponding to peaks of asymptomatic transmissions of 1%, 4%, 7% and 10%.

Table 4
Four transmission configurations of HPAI varying from direct contact transmission to indirect environmental transmission with two intermediate transmission routes, where one or the other mode of transmission is dominant. In all four cases, the parameters are set in order to have a cumulative infective peak of $I_H+A_H=9\%$. For example, the direct contact transmission leads to $p=p_2=0.041875$.

Case 1 *Only contact* $p=p_2$, $\varepsilon_H=0$	**Case 2** *Dominant contact* $p=0.03975$ (peak of 7.4% in isolation) and $\varepsilon_H = 1.56 \times 10^{-11}$ (no epidemic in isolation)
Case 3 *Only environmental* HPAI $p = 0$, $\varepsilon_H = 3.19 \times 10^{-10}$	**Case 4** *Dominant environmental* $p=0.003$ (no epidemic in isolation) $\varepsilon_H = 2.95 \times 10^{-10}$ (peak of 7% in isolation)

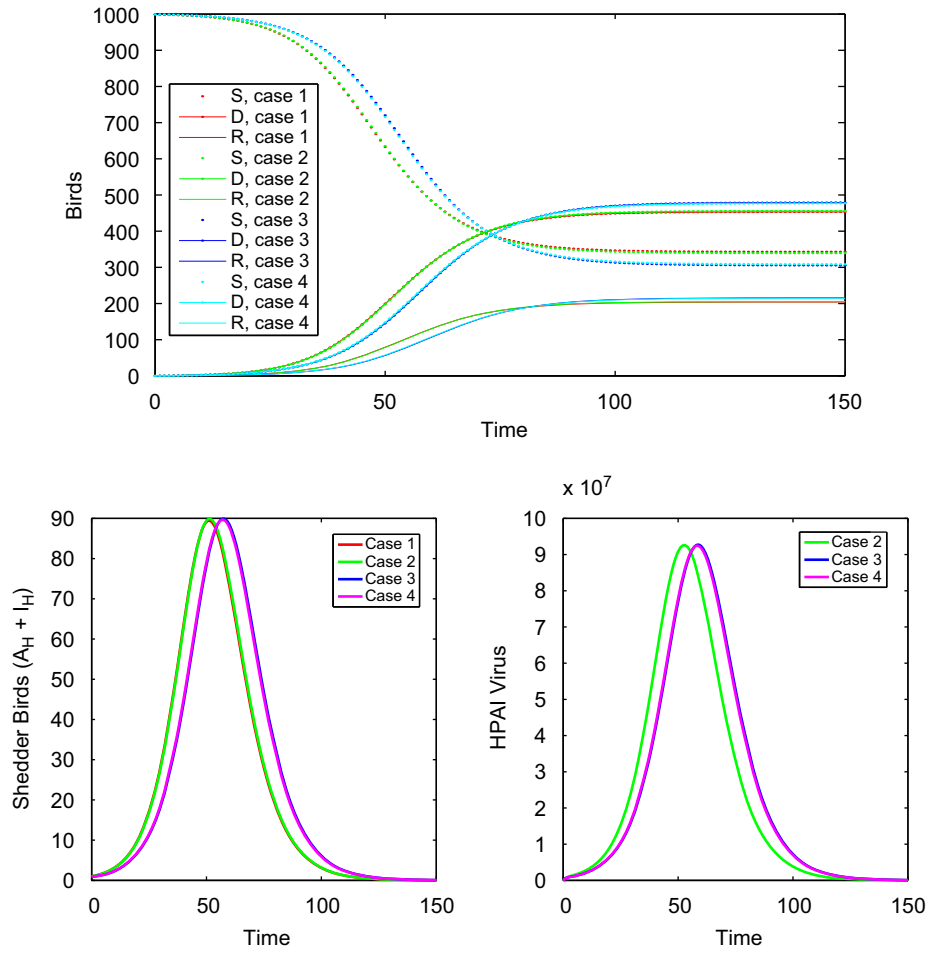

Fig. 13. Timeseries of (top) S, R_H and D, (bottom left) $A_H + I_H$, and (bottom right) V_H in the environment for the Cases 1, 2, 3, and 4 where only the HPAI strain is active. No LPAI strain virus is circulating and no LPAI infected individual is introduced.

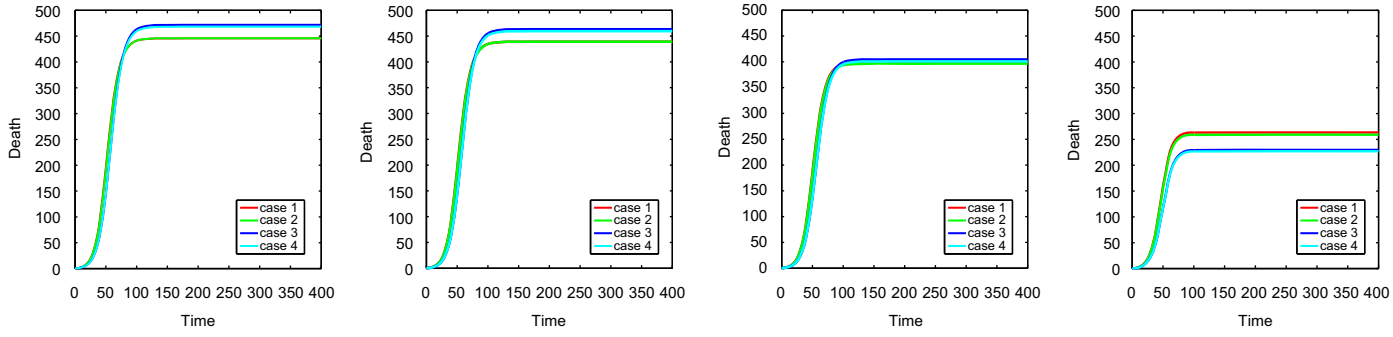

Fig. 14. Timeseries of the HPAI induced death for the full system with competing LPAI and HPAI strains and cases 1–4 of transmission modes of HPAI and increasing values LPAI incidence using values of ε_{L1}, ε_{L2}, ε_{L3}, and ε_{L4} (from left to right).

delay in the onset of local safety mechanisms and result in a worse epizootic when the effect of partial immunity wears off or when high doses of the shed virus reach fully naive flocks (naive to both LPAI and HPAI).

Acknowledgments

This work was supported by the Natural Sciences and Engineering Research Council of Canada, the Shared Hierarchical Academic Research Network, the Mathematics of Information Technology and Complex Systems, the Geomatics for Informed Decisions, and the Public Health Agency of Canada.

Appendix A. Reproduction numbers using the next generation matrix method

In this subsection we first use the next generation matrix method to estimate R_0 (Diekmann and Heesterbeek, 2000; van den Driessche and Watmough, 2002; Diekmann et al., 2009). Note that the decomposition between the rate of secondary infections and the rate of disease progression is not unique in this approach. There are two ways

in which individuals move into an infected compartment: (1) healthy individuals being infected; and (2) already infected individuals moving from one infected compartment to another. There is also an outgoing flow for each infected compartment. For a naive population completely susceptible to both strains, the disease-free equilibrium (DFE) of Eq. (1) corresponds to $E_0=(S^*,0,0,0,0,0,0,0,0)$, with $S^*=N$ the total number of birds (assumed to be constant). We will also consider another DFE with the proportion of the initial population that already went through an LPAI epidemic. In this latter configuration, assuming that the virus from the previous epidemic had time to be cleared from the environment, we will consider the DFE $E_1=(S^*,0,0,0,R_L^*,0,0,0,0)$, with $S^*+R_L^*=N$ constant.

A.1. At disease-free equilibrium E_0

The five components of the vector $\mathbb{F}$ representing the rate of secondary infections are

$$F_{A_L}=V_L\varepsilon_L S+r_L\varepsilon_L R_H V_L,$$

$$F_{A_H}=(\beta_A A_H+\beta_I I_H+\beta_{LH}A_{LH})S/N,$$

$$F_{I_H}=0,$$

$$F_{A_{LH}}=(\beta_A A_H+\beta_I I_H+\beta_{LH}A_{LH})R_L/N,$$

$$F_{V_L}=\phi_{A_L}A_L,$$

and the components of the vector $\mathbb{V}$ of rate of disease progression (difference between outgoing flow rate of infected individuals and all other incoming flow rates) are

$$V_{A_L}=\alpha_L A_L,$$

$$V_{A_H}=(\mu_{A_H}+\gamma_H)A_H,$$

$$V_{I_H}=(\mu_{I_H}+\alpha_H)I_H-\gamma_H A_H,$$

$$V_{A_{LH}}=\alpha_{LH}A_{LH},$$

$$V_V=\nu_L V_L.$$

The next generation matrix $K=FV^{-1}$, with matrices F and V such that $F_{i,j}=\partial\mathbb{F}_i/\partial x_j|_{E_0}$ and $V_{i,j}=\partial\mathbb{V}_i/\partial x_j|_{E_0}$, are evaluated at the disease-free equilibrium E_0. Following Diekmann and Heesterbeek (2000), we proceed to calculate the eigenvalues of K in search for the spectral radius:

$$F=\begin{pmatrix}0&0&0&0&\varepsilon_L S^*\\0&\beta_A S^*/N&\beta_I S^*/N&\beta_{LH}S^*/N&0\\0&0&0&0&0\\0&0&0&0&0\\\phi_{A_L}&0&0&0&0\end{pmatrix},$$

$$V=\begin{pmatrix}\alpha_L&0&0&0&0\\0&\gamma_H+\mu_{A_H}&0&0&0\\0&-\gamma_H&\mu_{I_H}+\alpha_H&0&0\\0&0&0&\alpha_{LH}&0\\0&0&0&0&\nu_L\end{pmatrix},$$

$$FV^{-1}=\begin{pmatrix}0&0&0&0&\frac{\varepsilon_L S^*}{\nu_L}\\0&\frac{\beta_A S^*/N}{\gamma_H+\mu_{A_H}}+\frac{\beta_I S^*/N\gamma_H}{(\gamma_H+\mu_{A_H})(\mu_{A_H}+\alpha_H)}&\frac{\beta_I S^*/N}{\mu_{I_H}+\alpha_H}&\frac{\beta_{LH}S^*/N}{\alpha_{LH}}&0\\0&0&0&0&0\\0&0&0&0&0\\\frac{\phi_{A_L}}{\alpha_L}&0&0&0&0\end{pmatrix}.$$

FV^{-1} eigenvalues:

$$\overline{R}_{0H1}=\frac{S^*/N\beta_I\gamma_H}{(\gamma_H+\mu_{A_H})(\mu_{I_H}+\alpha_H)}+\frac{\beta_A S^*/N}{\gamma_H+\mu_{A_H}},\quad \overline{R}_{0L1}=\sqrt{\frac{\varepsilon_L S^*\phi_{A_L}}{\nu_L\alpha_L}},$$

$$\overline{R}_{01}=0,\quad \overline{R}_{02}=0,\quad \overline{R}_{03}=-\sqrt{\frac{\varepsilon_L S^*\phi_{A_L}}{\nu\alpha_L}}.$$

A.2. Jacobian matrix

We derive threshold criteria from the linearized system about the disease-free equilibrium E_0. Consider $J_{i,j}=[\partial(Y)_i/\partial x_j]_{E_0}$ and the decoupling of the equation of R from the other variables leading to the Jacobian of the system of differential equations for the variables (S, A_L, A_H, I_L, I_H, R_L, R_H, A_{LH}, V_L) at the disease-free equilibrium E_0:

$$\mathbf{J}=\begin{pmatrix}0&0&-\beta_A S^*/N&-\beta_I S^*/N&0&0&-\beta_{LH}S^*/N&-\varepsilon_L S^*\\0&-\alpha_L&0&0&0&0&0&\varepsilon_L S^*\\0&0&\beta_A S^*/N-(\mu_{A_H}+\gamma_H)&\beta_I S^*/N&0&0&\beta_{LH}S^*/N&0\\0&0&\gamma_H&-(\mu_{I_H}+\alpha_H)&0&0&0&0\\0&0&0&0&0&0&0&0\\0&0&0&\alpha_H&0&0&0&0\\0&0&0&0&0&0&-\alpha_{LH}&0\\0&\phi_{A_L}&0&0&0&0&0&-\nu_L\end{pmatrix}.$$

The eigenvalues of the Jacobian at the disease-free equilibrium are

$$\lambda_1=\lambda_2=\lambda_3=0,\quad \lambda_4=-\alpha_{LH},$$

$$\lambda_5=-\tfrac{1}{2}\gamma_H+\tfrac{1}{2}\beta_A S^*/N-\tfrac{1}{2}\alpha_H-\tfrac{1}{2}\mu_{A_H}-\tfrac{1}{2}\mu_{I_H}+\tfrac{1}{2}\sqrt{(\beta_A S^*/N+\alpha_H+\mu_{I_H}-\gamma_H-\mu_{A_H})^2+4\gamma_H\beta_I S^*/N},$$

$$\lambda_6=-\tfrac{1}{2}\gamma_H+\tfrac{1}{2}\beta_A S^*/N-\tfrac{1}{2}\alpha_H-\tfrac{1}{2}\mu_{A_H}-\tfrac{1}{2}\mu_{I_H}-\tfrac{1}{2}\sqrt{(\beta_A S^*/N+\alpha_H+\mu_{I_H}-\gamma_H-\mu A_H)^2+4\gamma_H\beta_I S^*/N},$$

$$\lambda_7=-\tfrac{1}{2}(\nu_L+\alpha_L)+\tfrac{1}{2}\sqrt{(\nu_L-\alpha_L)+4\varepsilon_L S^*\phi_{A_L}},$$

$$\lambda_8=-\tfrac{1}{2}(\nu_L+\alpha_L)-\tfrac{1}{2}\sqrt{(\nu_L-\alpha_L)^2+4\varepsilon_L S^*\phi_{A_L}}.$$

A.3. The stability by the eigenvalues of the next generation matrix

We found above that the non-negative eigenvalues from the next generation matrix calculated around one of the disease-free equilibria $E_0=(S^*,0,0,0,0,0,0,0,0)$, with $S^*=N$ are

$$\overline{R}_{0H1}=\frac{S^*/N\beta_I\gamma_H}{(\gamma_H+\mu_{A_H})(\mu_{I_H}+\alpha_H)}+\frac{\beta_A S^*/N}{\gamma_H+\mu_{A_H}}\quad\text{and}\quad \overline{R}_{0L1}=\sqrt{\frac{\varepsilon_L S^*\phi_{A_L}}{\nu_L\alpha_L}}.$$

In addition, the two largest non-zero eigenvalues of the Jacobian matrix are

$$\lambda_5=-\tfrac{1}{2}\gamma_H+\tfrac{1}{2}\beta_A S^*/N-\tfrac{1}{2}\alpha_H-\tfrac{1}{2}\mu_{A_H}-\tfrac{1}{2}\mu_{I_H}+\tfrac{1}{2}\sqrt{(\beta_A S^*/N+\alpha_H+\mu_{I_H}-\gamma_H-\mu_{A_H})^2+4\gamma_H\beta_I S^*/N}$$

and

$$\lambda_7=-\tfrac{1}{2}(\nu_L+\alpha_L)+\tfrac{1}{2}\sqrt{(\nu_L-\alpha_L)^2+4\varepsilon_L S^*\phi_{A_L}}.$$

In the following, we assume $C=\gamma_H-\beta_A S^*/N+\alpha_H+\mu_{A_H}+\mu_{I_H}\geq 0$. This condition is always satisfied by the parameter values we used in this study. We have the following:

Theorem.

(i) $\overline{R}_{0H1}\geq 1\Leftrightarrow\lambda_5\geq 0$;
(ii) $\overline{R}_{0L1}\geq 1\Leftrightarrow\lambda_7\geq 0$.

In particular, if one of the $\overline{R}_{0H1}$ and $\overline{R}_{0L1}$ is larger than one, then the disease-free equilibrium E_0 is unstable.

Proof. $\lambda_5 \geq 0$ implies that

$$\sqrt{(\beta_A S^* + \alpha_H + \mu_{I_H} - \gamma_H - \mu_{A_H})^2 + 4\gamma_H \beta_I S^*/N} \geq \gamma_H - \beta_A S^*/N + \alpha_H + \mu_{A_H} + \mu_{I_H}.$$

Hence,

$$(\beta_A S^*/N + \alpha_H + \mu_{I_H} - \gamma_H - \mu_{A_H})^2 + 4\gamma_H \beta_I S^*/N \geq (\gamma_H - \beta_A S^*/N + \alpha_H + \mu_{A_H} + \mu_{I_H})^2,$$

and

$$4\gamma_H \beta_I S^*/N \geq (\gamma_H - \beta_A S^*/N + \alpha_H + \mu_{A_H} + \mu_{I_H})^2 - (\beta_A S^*/N + \alpha_H + \mu_{I_H} - \gamma_H - \mu_{A_H})^2$$

leading to

$$4\gamma_H \beta_I S^*/N \geq (2\gamma_H - 2\beta_A S^*/N + 2\mu_{A_H})(2\alpha_H + 2\mu_{I_H}).$$

Dividing both sides of the inequality by $4(\gamma_H + \mu_{A_H})(\alpha_H + \mu_{I_H})$ gives

$$\frac{\gamma_H \beta_I S^*/N}{(\gamma_H + \mu_{A_H})(\alpha_H + \mu_{I_H})} \geq 1 - \frac{\beta_A S^*/N}{\gamma_H + \mu_{A_H}} \quad \text{hence}$$
$$\frac{\gamma_H \beta_I S^*/N}{(\gamma_H + \mu_{A_H})(\alpha_H + \mu_{I_H})} + \frac{\beta_A S^*/N}{\gamma_H + \mu_{A_H}} \geq 1,$$

which is equivalent to $\overline{R}_{0H1} \geq 1$, showing that $\lambda_5 \geq 0 \Rightarrow \overline{R}_{0H1} \geq 1$.

Now we consider the reverse implication with $\overline{R}_{0H1} \geq 1$ leading to

$$\frac{\gamma_H \beta_I S^*/N}{(\gamma_H + \mu_{A_H})(\alpha_H + \mu_{I_H})} + \frac{\beta_A S^*/N}{\gamma_H + \mu_{A_H}} \geq 1.$$

Multiplying both sides by $(\gamma_H + \mu_{A_H})(\alpha_H + \mu_{I_H})$ results in

$$\gamma_H \beta_I S^*/N + \beta_A S^*/N(\alpha_H + \mu_{I_H}) \geq (\gamma_H + \mu_{A_H})(\alpha_H + \mu_{I_H}).$$

Hence,

$$\gamma_H \beta_I S^*/N \geq (\gamma_H + \mu_{A_H})(\alpha_H + \mu_{I_H}) - \beta_A S^*/N(\alpha_H + \mu_{I_H})$$

and

$$4\gamma_H \beta_I S^*/N \geq 4(\gamma_H + \mu_{A_H} - \beta_A S^*/N)(\alpha_H + \mu_{I_H}).$$

Thus,

$$4\gamma_H \beta_I S^*/N \geq (\gamma_H - \beta_A S^*/N + \alpha_H + \mu_{A_H} + \mu_{I_H})^2 - (\beta_A S^*/N + \alpha_H + \mu_{I_H} - \gamma_H - \mu_{A_H})^2$$

and

$$4\gamma_H \beta_I S^*/N + (\beta_A S^*/N + \alpha_H + \mu_{I_H} - \gamma_H - \mu_{A_H})^2 \geq (\gamma_H - \beta_A S^*/N + \alpha_H + \mu_{A_H} + \mu_{I_H})^2.$$

Under the condition $C = \gamma_H - \beta_A S^*/N + \alpha_H + \mu_{A_H} + \mu_{I_H} \geq 0$, we take the square root of both sides of the above inequality to obtain

$$\sqrt{4\gamma_H \beta_I S^*/N + (\beta_A S^*/N + \alpha_H + \mu_{I_H} - \gamma_H - \mu_{A_H})^2} \geq \gamma_H - \beta_A S^*/N + \alpha_H + \mu_{A_H} + \mu_{I_H},$$

or

$$-(\gamma_H - \beta_A S^* + \alpha_H + \mu_{A_H} + \mu_{I_H}) + \sqrt{4\gamma_H \beta_I S^* + (\beta_A S^* + \alpha_H + \mu_{I_H} - \gamma_H - \mu_{A_H})^2} \geq 0.$$

The left side is equal to λ_5. Thus, $\overline{R}_{0H1} \geq 1 \Rightarrow \lambda_5 \geq 0$ and this concludes the proof of $\overline{R}_{0H1} \geq 1 \Leftrightarrow \lambda_5 \geq 0$.

Similarly, we now show that $\overline{R}_{0L1} \geq 1 \Leftrightarrow \lambda_7 \geq 1$. First, $\lambda_7 \geq 0$ implies that

$$-\tfrac{1}{2}(\nu_L + \alpha_L) + \tfrac{1}{2}\sqrt{(\nu_L - \alpha_L)^2 + 4\phi_{A_L}\varepsilon_L S^*} \geq 0.$$

Thus,

$$(\nu_L - \alpha_L)^2 + 4\phi_{A_L}\varepsilon_L S^* \geq (\nu_L + \alpha_L)^2,$$

leading to

$$4\phi_{A_L}\varepsilon_L S^* \geq (\nu_L + \alpha_L)^2 - (\nu_L - \alpha_L)^2 \Longrightarrow 4\phi_{A_L}\varepsilon_L S^* \geq 4\alpha_L \nu_L.$$

Dividing both sides by $4\alpha_L \nu$ and taking the square root lead to

$$\sqrt{\frac{\phi_{A_L}\varepsilon_L S^*}{\alpha_L \nu_L}} \geq 1,$$

where the left side of the inequality is simply $\overline{R}_{0L1}$. Thus, we showed that $\lambda_7 \geq 0 \Rightarrow R_{0H1} \geq 1$. Showing the reverse implication is straightforward and does not lead to any condition on the choice of parameters. This completes the proof of $\overline{R}_{0L1} \geq 1 \Leftrightarrow \lambda_7 \geq 0$. □

A.4. At the disease-free equilibrium E_1

For a population that has a fraction of birds which went through an LPAI epidemic and are immunized to LPAI, the disease-free equilibrium has the form $E_1 = (S^*, 0, 0, 0, R_L^*, 0, 0, 0, 0)$, with $S^* + R_L^* = N$ the total constant population. The components of the vector $\mathbb{F}$ of the rate of secondary infections are

$$F_{A_L} = V_L \varepsilon_L S,$$

$$F_{A_H} = (\beta_A A_H + \beta_I I_H + \beta_{LH} A_{LH}) \frac{S}{N},$$

$$F_{I_H} = 0,$$

$$F_{A_{LH}} = (\beta_A A_H + \beta_I I_H + \beta_{LH} A_{LH}) \frac{R_L}{N},$$

$$F_V = \phi_{A_L} A_L,$$

and the components of the vector $\mathbb{V}$ of rate of disease progression (difference between outgoing flow rate of infected individuals and all other incoming flow rates) are

$$V_{A_L} = \alpha_L A_L,$$

$$V_{A_H} = (\mu_{A_H} + \gamma_H) A_H,$$

$$V_{I_H} = (\mu_{I_H} + \alpha_H) I_H - \gamma_H A_H,$$

$$V_{A_{LH}} = \alpha_{LH} A_{LH},$$

$$V_V = \nu_L V_L.$$

The next generation matrix $K = FV^{-1}$, with matrices F and V such that $F_{i,j} = \partial \mathbb{F}_i / \partial x_j|_{E_1}$ and $V_{i,j} = \partial \mathbb{V}_i / \partial x_j|_{E_1}$, are evaluated at the disease-free equilibrium E_1. We have

$$F = \begin{pmatrix} 0 & 0 & 0 & 0 & \varepsilon_L S^* \\ 0 & \beta_A \frac{S^*}{N} & \beta_I \frac{S^*}{N} & \beta_{LH} \frac{S^*}{N} & 0 \\ 0 & 0 & 0 & 0 & 0 \\ 0 & \beta_A \frac{R_L^*}{N} & \beta_I \frac{R_L^*}{N} & \beta_{LH} \frac{R_L^*}{N} & 0 \\ \phi_{A_L} & 0 & 0 & 0 & 0 \end{pmatrix},$$

$$V = \begin{pmatrix} \alpha_L & 0 & 0 & 0 & 0 \\ 0 & \gamma_H + \mu_{A_H} & 0 & 0 & 0 \\ 0 & -\gamma_H & \mu_{I_H} + \alpha_H & 0 & 0 \\ 0 & 0 & 0 & \alpha_{LH} & 0 \\ 0 & 0 & 0 & 0 & \nu_L \end{pmatrix},$$

$$FV^{-1}=\begin{pmatrix} 0 & 0 & 0 & 0 & \frac{\varepsilon_L S^*}{\nu_L} \\ 0 & \frac{\beta_A S^*}{N(\gamma_H+\mu_{A_H})}+\frac{\beta_I S^*\gamma_H}{N(\gamma_H+\mu_{A_H})(\mu_{A_H}+\alpha_H)} & \frac{\beta_I S^*}{N(\mu_{I_H}+\alpha_H)} & \frac{\beta_{LH}S^*}{N\alpha_{LH}} & 0 \\ 0 & 0 & 0 & 0 & 0 \\ 0 & \frac{\beta_A R_L^*}{N(\gamma_H+\mu_{A_H})}+\frac{\beta_I R_L^*\gamma_H}{N(\gamma_H+\mu_{A_H})(\mu_{A_H}+\alpha_H)} & \frac{\beta_I R_L^*}{N(\mu_{I_H}+\alpha_H)} & \frac{\beta_{LH}R_L^*}{N\alpha_{LH}} & 0 \\ \frac{\phi_{A_L}}{\alpha_L} & 0 & 0 & 0 & 0 \end{pmatrix}.$$

The eigenvalues of FV^{-1} are as follows:

$$\overline{R}_{0H2}=\frac{S^*\beta_I\gamma_H}{N(\gamma_H+\mu_{A_H})(\mu_{I_H}+\alpha_H)}+\frac{\beta_A S^*}{N(\gamma_H+\mu_{A_H})}+\frac{R_L^*\beta_{LH}}{N\alpha_{LH}}$$

$$\overline{R}_{0L2}=\sqrt{\frac{\varepsilon_L S^*\phi_{A_L}}{\nu_L\alpha_L}},$$

$$\overline{R}_{01}=0,\quad \overline{R}_{02}=0,\quad \overline{R}_{03}=-\sqrt{\frac{\varepsilon_L S^*\phi_{A_L}}{\nu_L\alpha_L}}.$$

The epidemiological interpretation of $\overline{R}_{0H2}$ and $\overline{R}_{0L2}$ are given in the main text.

Appendix B. Environmental transmission of HPAI

B.1. Model

$$\dot{S}=-\varepsilon_L V_L S-\varepsilon_H V_H S-(\beta_A(A_{He}+A_{Hc})+\beta_I(I_{He}+I_{Hc})+\beta_{LH}(A_{LHe}+A_{LHc}))S/N,$$

$$\dot{A}_L=\varepsilon_L V_L S-\alpha_L A_L,$$

$$\dot{A}_{He}=S\varepsilon_H V_H-\mu_{A_H}A_{He}-\gamma_H A_{He},$$

$$\dot{A}_{Hc}=\beta_A(A_{He}+A_{Hc})+\beta_I(I_{He}+I_{Hc})+\beta_{LH}(A_{LHe}+A_{LHc}))S/N-\mu_{A_H}A_H-\gamma_H A_{Hc},$$

$$\dot{I}_{He}=\gamma_H A_{He}-\mu_{I_H}I_{He}-\alpha_H I_{He},$$

$$\dot{I}_{Hc}=\gamma_H A_{Hc}-\mu_{I_H}I_{Hc}-\alpha_H I_{Hc},$$

$$\dot{R}_L=\underbrace{\alpha_L A_L}_{\text{recovery from LPAI}}-\underbrace{(\beta_A(A_{He}+A_{Hc})+\beta_I(I_{He}+I_{Hc})+\beta_{LH}(A_{LHe}+A_{LHc}))R_L/N-\varepsilon_H R_L V_H}_{\text{2nd infection by HPAI strain}},$$

$$\dot{R}_H=\underbrace{\alpha_H I_{He}+\alpha_H I_{Hc}}_{\text{recovery from HPAI}},$$

$$\dot{A}_{LHe}=\varepsilon_H R_L V_H-\alpha_{LH}A_{LHe},$$

$$\dot{A}_{LHc}=(\beta_A(A_{He}+A_{Hc})+\beta_I(I_{He}+I_{Hc})+\beta_{LH}(A_{LHe}+A_{LHc}))R_L/N-\alpha_{LH}A_{LHc},$$

$$\dot{R}=\underbrace{\mu_{A_H}(A_{He}+A_{Hc})+\mu_{I_H}(I_{He}+I_{Hc})}_{\text{disease induced death}}+\underbrace{\alpha_{LH}(A_{LHe}+A_{LHc})}_{\text{recovery from HPAI}},$$

$$\dot{V}_L=\phi_{A_L}A_L-\nu_L V_L,$$

$$\dot{V}_H=\phi_{A_H}(A_{He}+A_{Hc})+\phi_{I_H}(I_{He}+I_{Hc})+\phi_{A_{LH}}(A_{LHe}+A_{LHc})-\nu_H V_H.$$

Here the variables are similar to those displayed in Table 1, with the additional subscripts e and c, representing environmental and contact, respectively. The additional variable of the system is V_H, which tracks the amount of infectious doses of HPAI virus in the environment. The separation of populations into those infected via contact and those infected via environmental sources is only done for the HPAI strain as we continue to assume a dominant environmental transmission of the LPAI strain. The values of the parameters are discussed in the following section.

B.2. Data and parameter estimation

First, note that the HPAI bird infection dose (b.i.d) is lower than that of LPAI, with $\omega_H=10^{0.95}$ EID_{50}/ml (Brown et al., 2007). The number of infectious doses produced by a symptomatic HPAI infected bird was not found directly in the literature. Here we show how we estimated this parameter ϕ_{I_H} based on the available data. Obtaining the estimate of the HPAI virus load in the feces of HPAI infected birds was difficult due to the disparity in units and methods of measurements of HPAI virus shedding in the biological literature. Hence, we assume that for a given virus strain, the density of virions in the feces is proportional to the concentration of virions found after dilution of cloacal swabs i.e. $X_{LPAI}/X_{HPAI}=CS_{LPAI}/CS_{HPAI}$, where CS_i is the cloacal virus concentration for strain i per 1 ml and X_i is the amount of virions per gram of feces. The average amount of LPAI virions per gram of feces is $X_{LPAI}=10^{8.7}$ EID_{50}/g (Webster et al., 1992) and we extract the concentration of LPAI virus in cloacal swab from the results of Spackman et al. (2007). Note, however, that pekin ducks are used for this estimation. These birds are reported to be slightly more vulnerable to LPAI than wood ducks. As a result, we expect our result to be a slight overestimation of the HPAI virus concentration in the feces of wood ducks. Spackman et al. (2007) found cloacal swabs of LPAI H5N1 in pekin ducks, and estimated the average of $CS_{LPAI}=10^{4.75}$ EID_{50}/ml. In addition, Brown et al. (2006) found a cloacal shedding of HPAI strain (peak titers) $C_{HPAI}=10^{3.8}$ EID_{50}/ml (Mongolia/05) for wood ducks. We assume that the peak titer is associated with the shedding in the infectious stage of our model (I_H). Consider the data of the Mongolia/05 strain we obtain $10^{4.75}EID_{50}/ml/10^{3.8}EID_{50}/ml=10^{8.7}EID_{50}/g/X_{HPAI}$. Thus, $X_{HPAI}=10^{7.75}EID_{50}/g$ and hence, $\phi_{I_H}=10^{8.75}\times 10^3\times X_{HPAI}/(\omega_H\times 365)=10^{8.18}$ day^{-1}, where the average value of $10^{8.75}\times 10^3/365$ grams of feces per day was used (WHO-EPAR, 2009).

We end up with $\phi_{A_H}=\phi_{I_H}/1.75$ and $\phi_{A_{LH}}=\phi_{I_H}/2.0$ (see Kalthoff et al., 2008). Finally, the virus survival parameter is based on the survival of HPAI for an average of 28 days and LPAI for an on average of 39.375 days (Brown et al., 2007). Hence, we consider $\nu_H/\nu_L=\frac{39.375}{28.0}$, leading to $\nu_H=\nu_L\frac{39.375}{28.0}=1.23$ day^{-1}.

References

Alexander, D.J., 2007. An overview of the epidemiology of avian influenza. Vaccine 25, 5637–5644.

Andreasen, V., Lin, J., Levin, S.A., 1997. The dynamics of cocirculating influenza strains conferring partial cross-immunity. J. Math. Biol. 35, 825–842.

Bourouiba, L., Wu, J., Newman, S., Takekawa, J., Natdorj, T., Batbayar, N., Bishop, C.M., Hawkes, L.A., Butler, P.J., Wikelski, M., 2010. Spatial dynamics of bar-headed geese migration in the context of H5N1. J. R. Soc. Interface 7, 1627–1639.

Brauer, F., van den Driessche, P., Wu, J. (Eds.), 2008. Mathematical Epidemiology. Lecture Notes in Mathematics. Springer.

Breban, R., Drake, J.M., Stallknecht, D.E., Rohani, P., 2009. The role of environmental transmission in recurrent avian influenza epidemics. PLoS Comput. Biol. 5 e1000346-1–11.

Brown, J.D., Goekjian, G., Poulson, R., Valeika, S., Stallknecht, D.E., 2009. Avian influenza virus in water: infectivity is dependent on pH, salinity and temperature. Vet. Microbiol. 136, 20–26.

Brown, J.D., Stallknecht, D.E., Beck, J.R., Suarez, D.L., Swayne, D.E., 2006. Susceptibility of North American ducks and gulls to H5N1 highly pathogenic avian influenza viruses. Emerg. Infect. Dis. 12, 1663–1670.

Brown, J.D., Stallknecht, D.E., Swayne, D.E., 2008. Experimental infection of swans and geese with highly pathogenic avian influenza virus (H5N1) of Asian lineage. Emerg. Infect. Dis. 14, 136–142.

Brown, J.D., Swayne, D.E., Cooper, R.J., Burns, R.E., Stallknecht, D.E., 2007. Persistence of H5 and H7 avian influenza viruses in water. Avian Dis. 51, 285–289.

CDC, 2006. Centers for disease control & prevention on avian influenza: current situation. Centers for Disease Control. URL ⟨http://www.cdc.gov/flu/avian/outbreaks/current.htm⟩.

Diekmann, O., Heesterbeek, J.A.P., Roberts, M.G., 2009. The construction of next-generation matrices for compartmental epidemic models. In: Ed., Simon Levin, Journal of Royal Society Interface. Wiley series in Mathematical and Computational Biology, Princeton University, USA.

Diekmann, O., Heesterbeek, J.A.P., Roberts, M.G., 2009. The construction of next-generation matrices for compartmental epidemic models. J. R. Soc. Interface.

Gilbert, M., Xiao, X., Pfeiffer, D.U., Epprecht, M., Boles, S., Czarnecki, C., Chaitaweesub, P., Kalpravidh, W., Minh, P.Q., Otte, M.J., Martin, V., Slingenbergh, J., 2008.

Mapping H5N1 highly pathogenic avian influenza risk in Southeast Asia. Proc. Natl. Acad. Sci. 105, 4769–4774.
Globig, A., Staubach, C., Beer, M., Köppen, U., Fiedler, W., Nieburg, M., Wilking, H., Starick, E., Teifke, J.P., Werner, O., Unger, F., Grund, C., Wolf, C., Roost, H., Feldhusen, F., Conraths, F.J., Mettenleiter, T.C., Harder, T.C., 2009. Epidemiological and ornithological aspects of outbreaks of highly pathogenic avian influenza virus H5N1 of Asian lineage in wild birds in Germany, 2006 and 2007. Transboundary Emerg. Dis. 56, 57–72.
Heffernan, J.M., Smith, R.J., Wahl, L.M., 2005. Perspectives on the basic reproduction ratio. J. R. Soc. Interface 2, 281–293.
Iwami, S., Takeuchi, Y., Liu, X., Nakaoka, S., 2009. A geographical spread of vaccine-resistance in avian influenza epidemics. J. Theor. Biol. 259, 219–228.
Jeong, O.-M., Kim, M.-C., Kang, H.-M., Kim, H.-R., Kim, Y.-J., Joh, S.-J., Kwon, J.-H., Lee, Y.-J., 2009. Experimental infection of chickens, ducks and quails with the highly pathogenic H5N1 avian influenza virus. J. Vet. Sci. 10, 53–60.
Kalthoff, D., Breithaupt, A., Teifke, J.P., Globig, A., Harder, T., Mettenleiter, T.C., et al., 2008. Pathogenicity of highly pathogenic avian influenza virus (H5N1) in adult mute swans. Emerg. Infect. Dis. 14, 1267–1270.
Keawcharoen, J., van Riel, D., van Amerongen, G., Bestebroer, T., Beyer, W.E., van Lavieren, R., et al., 2008. Wild ducks as long-distance vectors of highly pathogenic avian influenza virus (H5N1). Emerg. Infect. Dis. 14, 600–607.
Lucchetti, J., Roy, M., Martcheva, M., 2009. An avian influenza model and its fit to human avian influenza cases, 1–30. Advances in Disease Epidemiology, Jean Michel Tchuenche and Zindoga Mukandavire (Eds.), Nova Science Publishers — March 2010, 160741452X : 9781607414520.
Munster, V., Baas, C., Lexmond, P., Waldenström, J., Wallensten, A., et al., 2007. Temporal, and species variation in prevalence of influenza a viruses in wild migratory birds. PLoS Pathog. 13.
Pasick, J., Berhane, Y., Embury-Hyatt, C., et al., 2007. Susceptibility of Canada geese to highly pathogenic avian influenza virus. Emerg. Infect. Dis. 13.
Rohania, P., Brebana, R., Stallknechte, D.E., Drakea, J.M., 2009. Environmental transmission of low pathogenicity avian influenza viruses and its implications for pathogen invasion. Proc. Natl. Acad. Sci. 106, 10365–10369.
Schaefer, J.M., Cohen, J., Hostetle, M.E., 2009. The wood duck. UF/IFAS EDIS Web. URL ⟨http://edis.ifas.ufl.edu/uw180#FOOTNOTE_2⟩.
Seo, S.H., Webster, R.G., 2001. Cross-reactive, cell-mediated immunity and protection of chickens from lethal H5N1 influenza virus infection in Hong Kong poultry markets. J. Virol. 75, 2516–2525.
Spackman, E., Swayne, D.E., Suarez, D.L., Senne, D.A., Pedersen, J.C., Killian, M.L., Pasick, J., Handel, K., Somanathan Pillai, S.P., Lee, C.-W., Stallknecht, D., Slemons, R., Ip, H.S., Deliberto, T., 2007. Characterization of low pathogenicity H5N1 avian influenza viruses from North America. J. Virol. 81 (21), 11612–11619.
Stallknecht, D.E., 1997. Ecology and epidemiology of avian influenza viruses in wild bird populations: waterfowl, shorebirds, pelicans, cormorants, etc. Avian Dis. 47, 61–69.
Stallknecht, D.E., Brown, J.D., 2007. Wild birds and the epidemiology of avian influenza. J. Wild Life Dis. 43, S15–S20.
Swayne, D., Suarez, D., 2000. Highly pathogenic avian influenza. Rev. Sci. Tech. 19, 463–482.
van den Driessche, P., Watmough, J., 2002. Reproduction numbers and subthreshold endemic equilibria for compartmental models of disease transmission. Math. Biosci. 180, 29–48.
Webster, R., Bean, W., Gorman, O., Chambers, T., Kawaoka, Y., 1992. Evolution and ecology of influenza a viruse. Macrobiol. Rev. K 56 (March), 152–179.
WHO, 2008. Avian influenza situation in Pakistan—update 2. Technical Report, World Health Organization. URL ⟨http://www.who.int/csr/don/2008_04_03/en/index.html⟩.
WHO-EPAR, 2009. H5N1 avian influenza: timeline of major events. Technical Report, World Health Organization, Epidemic and Pandemic Alert and Response. URL ⟨http://www.who.int/csr/disease/avian_influenza/ai_timeline/en/⟩.
WHO, Mar 2010. World Health Organization. Cumulative number of confirmed human cases of avian influenza a/(H5N1) reported to who. URL ⟨http://www.who.int/csr/disease/avian_influenza/country/cases_table_2010_03_16/en/index.html⟩.